

1

AD-A214 734

ESL-TR-88-56

GRAVITY EFFECTS IN SMALL-SCALE STRUCTURAL MODELING: ANALYTICAL AND EXPERIMENTAL APPROACH

Y.S. KIM, H.P. POA, S.C. LING

GENERAL TECHNOLOGY, INC.
500 NORCROSS WAY
SILVER SPRING MD 20904

APRIL 1988

FINAL REPORT

AUGUST 1987 — MARCH 1988

DTIC
ELECTE
NOV 3 1989
S B D
Co

APPROVED FOR PUBLIC RELEASE: DISTRIBUTION UNLIMITED



ENGINEERING & SERVICES LABORATORY
AIR FORCE ENGINEERING & SERVICES CENTER
TYNDALL AIR FORCE BASE, FLORIDA 32403

88 11 00 047

NOTICE

PLEASE DO NOT REQUEST COPIES OF THIS REPORT FROM
HQ AFESC/RD (ENGINEERING AND SERVICES LABORATORY).

ADDITIONAL COPIES MAY BE PURCHASED FROM:

NATIONAL TECHNICAL INFORMATION SERVICE
5285 PORT ROYAL ROAD
SPRINGFIELD, VIRGINIA 22161

FEDERAL GOVERNMENT AGENCIES AND THEIR CONTRACTORS
REGISTERED WITH DEFENSE TECHNICAL INFORMATION CENTER
SHOULD DIRECT REQUESTS FOR COPIES OF THIS REPORT TO:

DEFENSE TECHNICAL INFORMATION CENTER
CAMERON STATION
ALEXANDRIA, VIRGINIA 22314

REPORT DOCUMENTATION PAGE				Form Approved OMB No 0704-0188	
1a. REPORT SECURITY CLASSIFICATION UNCLASSIFIED		1b. RESTRICTIVE MARKINGS			
2a. SECURITY CLASSIFICATION AUTHORITY		3. DISTRIBUTION/AVAILABILITY OF REPORT Approved for public release. Distribution unlimited.			
2b. DECLASSIFICATION/DOWNGRADING SCHEDULE					
4. PERFORMING ORGANIZATION REPORT NUMBER(S) GTI Report No. 88-03		5. MONITORING ORGANIZATION REPORT NUMBER(S) ESL-TR-88-56			
6a. NAME OF PERFORMING ORGANIZATION General Technology, Inc.		6b. OFFICE SYMBOL (If applicable)	7a. NAME OF MONITORING ORGANIZATION Air Force Engineering and Services Center (RDGS)		
6c. ADDRESS (City, State, and ZIP Code) 500 Norcross Way Silver Spring, MD 20904		7b. ADDRESS (City, State, and ZIP Code) HQ AFESC/RDGS Tyndall AFB, FL 32403			
8a. NAME OF FUNDING SPONSORING ORGANIZATION		8b. OFFICE SYMBOL (If applicable)	9. PROCUREMENT INSTRUMENT IDENTIFICATION NUMBER Contract # F08635-87-C-0445		
8c. ADDRESS (City, State, and ZIP Code)		10. SOURCE OF FUNDING NUMBERS			
		PROGRAM ELEMENT NO 65502F	PROJECT NO 3005	TASK NO 0016	WORK UNIT ACCESSION NO
11. TITLE (Include Security Classification) (U) Gravity Effects in Small-Scale Structural Modeling: Analytical and Experimental Approach					
12. PERSONAL AUTHOR(S) Y. S. Kim, H. P. Poa, S. C. Ling					
13a. TYPE OF REPORT Final Technical Report		13b. TIME COVERED FROM 870821 TO 880331	14. DATE OF REPORT (Year, Month, Day) 1988 Apr		15. PAGE COUNT 67
16. SUPPLEMENTARY NOTATION Availability of this report is specified on reverse of front cover.					
17. COSATI CODES			18. SUBJECT TERMS (Continue on reverse if necessary and identify by block number)		
FIELD	GROUP	SUB-GROUP	Rayleigh Waves		
08	13		Impact Energy		
13	02		Dynamic Loading		
			Gravity Potential Energy		
			Strain Energy		
			Small-scale Modeling		
19. ABSTRACT (Continue on reverse if necessary and identify by block number) An analytical investigation and laboratory study on gravity effects in small-scale modeling have been performed. The appropriate scaling length for ground movement is identified as $t=G/(pg)$, when gravity effects are important. Dimensionless gravity parameter, $pg\lambda/G$, and impact energy parameter, $WH/(G\lambda^3)$, are identified as the key governing parameters for the problem. Laboratory techniques and procedures have been developed for compensating gravity effect without using artificially induced gravity. Experimental results were summarized in twelve tables and twelve graphs.					
20. DISTRIBUTION/AVAILABILITY OF ABSTRACT <input checked="" type="checkbox"/> UNCLASSIFIED/UNLIMITED <input type="checkbox"/> SAME AS RPT <input type="checkbox"/> DTIC USERS			21. ABSTRACT SECURITY CLASSIFICATION		
22a. NAME OF RESPONSIBLE INDIVIDUAL Capt I. J. Schantz		22b. TELEPHONE (Include Area Code) (904) 283-6237		22c. OFFICE SYMBOL HQ AFESC/RDGS	

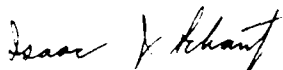
PREFACE

This report was prepared by General Technology, Inc., 500 Norcross Way, Silver Spring, MD 20904, under contract F08635-87-C-0445, for the Air Force Engineering and Services Center (AFESC), Tyndall Air Force Base, Florida. The report summarizes work done between August 1987 and March 1988. Lt Col Robert Majka and Capt Isaac Schantz were the Air Force project officers.

This report has been reviewed by the Public Affairs Office and is releasable to the National Technical Information Service (NTIS). At NTIS, it will be available to the general public, including foreign nations.

This technical report was submitted as part of the Small Business Innovative Research (SBIR) Program and has been published according to SBIR directives in the format in which it was submitted.

This technical report has been reviewed and is approved for publication.


ISAAC J. SCHANTZ, Capt, USAF
Research Mechanical Engineer


WILLIAM S. STRICKLAND
Chief, Structures and Weapons
Effects Branch


ROBERT J. MAJKA, Lt Col, USAF
Chief, Engineering Research
Division


LAWRENCE D. HOKANSON, Colonel, USAF
Director, Engineering and Services
Laboratory

TABLE OF CONTENTS

Section	Title	Page
I	INTRODUCTION	1
	A. OBJECTIVE	1
	B. BACKGROUND	1
	C. SCOPE	2
II	WAVE PROPOGATION IN SOLIDS	3
	A. INTRODUCTION	3
	B. EQUATION OF MOTION IN AN ELASTIC MEDIUM WITHOUT GRAVITY FORCE	3
	C. EQUATION OF MOTION IN AN ELASTIC MEDIUM WITH GRAVITY FORCE	16
III	LABORATORY INVESTIGATION	21
	A. INTRODUCTION	21
	B. DESCRIPTION OF TESTING FACILITY AND MODEL	24
	C. LABORATORY PROGRAM	28
IV	LABORATORY RESULTS	32
	A. THE INFLUENCE OF SHEAR MODULUS OF SOLID AND IMPACT LOADINGS	32
V	CONCLUSIONS AND RECOMMENDATIONS	58
	A. CONCLUSIONS	58
	B. RECOMMENDATIONS	59
	REFERENCES	61

1/22/52
2

v

Accession For	
NTIS GRA&I	<input checked="" type="checkbox"/>
DTIC TAB	<input type="checkbox"/>
Unannounced	<input type="checkbox"/>
Justification	
By _____	
Distribution/ _____	
Availability Codes	
Dist	Avail and/or Special
A-1	

LIST OF FIGURES

Figure	Title	Page
1	Notations for Normal and Shear Stresses in Cartesian Coordinates System	4
2	Derivation of the Equation of Motion in an Elastic Medium	4
3	Amplitude Ratio vs. Dimensionless Depth for Rayleigh Wave	17
4	Photograph of Velocity and Pressure Transducers	26
5	Photograph of Model, Recorder, and Impact Loading System ..	27
6	Photograph of Shear Loading Apparatus	29
7	Photograph of Aluminium Drop Weights	30
8	Pressure and Velocity Responses for a Model with H = 1 in., ϕ = 3 in., W = 0.4 lb. and G = 0.2 psi	33
9	Pressure and Velocity Responses for a Model with H = 1 in., ϕ = 3 in., W = 0.4 lb. and G = 1.4 psi	33
10	Wavelength vs. Prop Height for Models with G = 0.2 psi	47
11	Wavelength vs. Prop Height for Models with G = 1.4 psi	48
12	Wave Speed vs. Drop Height for Models with G = 0.2 psi	50
13	Wave Speed vs. Drop Height for Models with G = 1.4 psi	51
14	A Relationship of Dimensionless Parameters for Models with G = 0.2 psi	52
15	A Relationship of Dimensionless Parameters for Models with G = 1.4 psi	52
16	Maximum Pressure vs. Impact Energy for Models with G = 0.2 psi	54

LIST OF FIGURES
(concluded)

Figure	Title	Page
17	Maximum Pressure vs. Impact Energy for Models with G = 1.4 psi	55
18	Maximum Velocity vs. Impact Energy for Models with G = 0.2 psi	56
19	Maximum Velocity vs. Impact Energy for Models with G = 1.4 psi	57

LIST OF TABLES

Table	Title	Page
1	Variation of the Ratio of the Rayleigh to the Shear Wave for Various Poisson's Ratio	15
2	Parameters Considered in the Model Tests	31
3	Test Results for Model 1	35
4	Test Results for Model 2	36
5	Test Results for Model 3	37
6	Test Results for Model 4	38
7	Test Results for Model 5	39
8	Test Results for Model 6	40
9	Test Results for Model 7	41
10	Test Results for Model 8	42
11	Test Results for Model 9	43
12	Test Results for Model 10	44
13	Test Results for Model 11	45
14	Test Results for Model 12	46

SECTION I
INTRODUCTION

A. OBJECTIVES

The primary objective of this study was to investigate the gravitational effects in an elastic medium. More specifically, the objectives of this study were to: (1) derive a governing equation of the motion with gravity force term, (2) develop an experimental technique to simulate the gravitational effects, (3) determine the parameters that govern the gravitational effects in an elastic medium using a model technique in the laboratory, and (4) gain experience necessary for detailed model studies in the Phase II Program.

B. BACKGROUND

Many studies have been performed to investigate the soil-structure interaction problems subjected to dynamic loading conditions. Research work simulating this problem used either full-scale or small-scale laboratory modeling techniques. The full-scale technique with the necessary instrumentation (i.e., soil stress meters, pore water pressure transducers, settlement gauges, and strain gauges, etc.) gave the best results for estimating prototype behavior. However, this technique has shown serious major drawbacks: mainly, cost and time of construction and operation. For these reasons, **small-scale modeling has been used as an alternate testing method.**

However, the use of small-scale modeling in the laboratory has shown severe limitation when the gravity body force of the structure

itself is the principal load on the system. This is because: (1) soil characteristics are nonlinear and overburden dependent, and (2) smaller stress magnitudes. The stresses in a small-scale model due to its own weight are much smaller in magnitude than those in the corresponding prototype system. Because of this limitation, the effects of the gravity has been neglected in the small-scale model technique based on the assumption that gravitational and strain rate effects are insignificant.

In recent years, however, a new model technique (centrifuge model technique) has been introduced and applied to small-scale models to simulate gravitational effects. Based on the centrifuge model studies (References 4, 10 & 11), it has been demonstrated that the gravity scale is an important parameter in small-scale model study. The purpose of this research was therefore, to determine the parameters that govern the gravitational effects without using the centrifuge model technique.

C. SCOPE

This contains a review of elastic waves in a solid medium without gravity force; a derivation of a governing differential equation of the motion with gravity force; a description of developed laboratory testing facility; and preliminary model test results and discussion. Finally, conclusion are drawn and used to offer recommendations for the direction of future research.

SECTION II

WAVE PROPOGATION IN SOLIDS

A. INTRODUCTION

Dynamic load-generated waves can be divided into three main categories: compressive, shear, and surface. The three main wave types can be divided into two varieties: body waves, which propagate through the body of soil, and surface waves, which are transmitted along a surface. The most important surface wave is Rayleigh's wave. Body waves can be further subdivided into compressive or longitudinal waves, and distortional or shear waves. This section reviews these three types of wave.

B. EQUATION OF MOTION IN AN ELASTIC MEDIUM WITHOUT GRAVITY FORCE

Figure 1 shows an isotropic elastic medium whose sides measure dx and dy . The normal stress acting on the planes normal to the x and y axes are σ_x and σ_y , respectively. The shear stresses are τ_{xy} and τ_{yx} .

Let u and v be the displacements in the direction of x and y , respectively. Then the expressions for strains and rotations of the medium are:

$$\epsilon_x = \frac{\partial u}{\partial x} \dots \dots \dots (1)$$

$$\epsilon_y = \frac{\partial v}{\partial y} \dots \dots \dots (2)$$

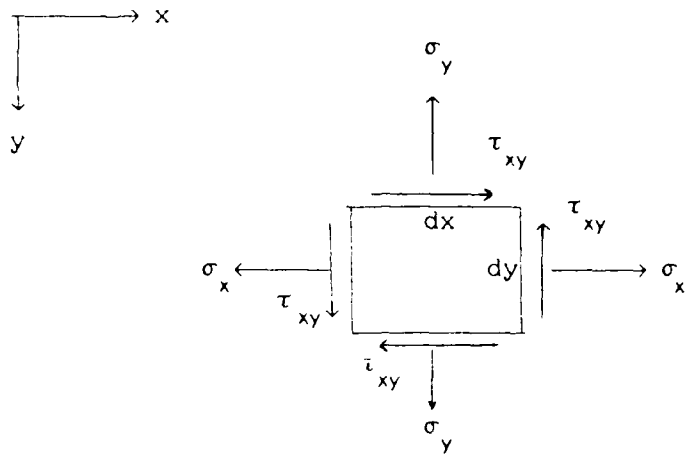


Figure 1. Notations for Normal and Shear stresses in Cartesian Coordinates System

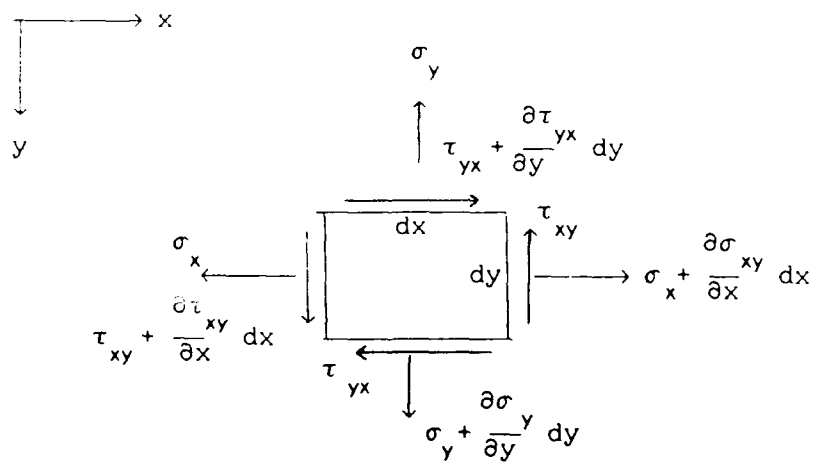


Figure 2. Derivation of the Equations of Motion in an Elastic Medium

$$\gamma_{xy} = \frac{\partial v}{\partial x} + \frac{\partial u}{\partial y} \dots \dots \dots (3)$$

$$2\bar{\omega} = \frac{\partial v}{\partial x} - \frac{\partial u}{\partial y} \dots \dots \dots (4)$$

where ,

ϵ_x and ϵ_y = normal strains in the direction of
x and y, respectively,

γ_{xy} = shearing strain, and

$\bar{\omega}$ = the components of rotation about the
x and y axes

The generalized Hooke's law is used for the relationship between stresses and strains:

$$\epsilon_x = \frac{1}{E} (\sigma_x - \nu \sigma_y) \dots \dots \dots (5)$$

$$\epsilon_y = \frac{1}{E} (\sigma_y - \nu \sigma_x) \dots \dots \dots (6)$$

$$\tau_{xy} = G \cdot \gamma_{xy} \dots \dots \dots (7)$$

where E is Young's Modulus, ν is Poisson's Ratio, and G is shear modulus defined as $G = E / (2 (1 + \nu))$.

Equations (5) and (6) can be rewritten in terms of normal strains as:

$$\sigma_x = \lambda \cdot \bar{\epsilon} + 2G \cdot \epsilon_x \dots\dots\dots (8)$$

$$\sigma_y = \lambda \cdot \bar{\epsilon} + 2G \cdot \epsilon_y \dots\dots\dots (9)$$

where,

$$\lambda = \nu \cdot E / ((1+\nu)(1-\nu)) \dots\dots\dots (10)$$

$$\bar{\epsilon} = \epsilon_x + \epsilon_y = \text{volumetric strain.}$$

To obtain the equation of motion for an elastic medium, stresses acting on an element with sides measuring dx and dy are considered as shown in Figure 2. Four separate forces will be acting parallel to each axis, and if one considers the resultant force acting in the x-direction:

$$\left(-\sigma_x + \left(\sigma_x + \frac{\partial \sigma_x}{\partial x} dx \right) \right) dy + \left(-\tau_{yx} + \left(\tau_{yx} + \frac{\partial \tau_{yx}}{\partial y} dy \right) \right) dx$$

which simplifies to

$$\left(\frac{\partial \sigma_x}{\partial x} + \frac{\partial \tau_{yx}}{\partial y} \right) dx dy$$

and by the Newton's second law of motion, neglecting body forces such as gravity, this will be equal to $(\rho dx dy (\partial^2 u / \partial t^2))$ where ρ is density of the element, so that

$$\frac{\partial \sigma_x}{\partial x} + \frac{\partial \tau_{yx}}{\partial y} = \rho \frac{\partial^2 u}{\partial t^2} \dots\dots\dots (11)$$

Similarly,

$$\frac{\partial \sigma_y}{\partial y} + \frac{\partial \tau_{xy}}{\partial x} = \rho \frac{\partial^2 v}{\partial t^2} \dots \dots \dots (12)$$

These equations of motion will hold, whatever the stress-strain behavior of the medium. In order to solve the equations, let us substitute Equations (7) and (8) into the Equation (11).

It yields

$$\rho \frac{\partial^2 u}{\partial t^2} = \frac{\partial}{\partial x} (\lambda \bar{\epsilon} + 2G \cdot \epsilon_x) + G \frac{\partial}{\partial y} \left(\frac{\partial v}{\partial x} + \frac{\partial u}{\partial y} \right)$$

or

$$\rho \frac{\partial^2 u}{\partial t^2} = \lambda \frac{\partial \bar{\epsilon}}{\partial x} + G \left(\frac{\partial^2 u}{\partial x^2} + \frac{\partial^2 v}{\partial x \partial y} + \frac{\partial^2 u}{\partial x^2} + \frac{\partial^2 u}{\partial y^2} \right)$$

Since

$$\frac{\partial^2 u}{\partial x^2} + \frac{\partial^2 v}{\partial x \partial y} = \frac{\partial \bar{\epsilon}}{\partial x} ,$$

the equation of the motion becomes

$$\rho \frac{\partial^2 u}{\partial t^2} = (\lambda + G) \frac{\partial \bar{\epsilon}}{\partial x} + G \cdot \nabla^2 u \dots \dots \dots (13)$$

where

$$\nabla^2 = \frac{\partial^2}{\partial x^2} + \frac{\partial^2}{\partial y^2}$$

Similarly,

$$\rho \frac{\partial^2 v}{\partial t^2} = (\lambda + G) \frac{\partial \bar{\epsilon}}{\partial y} + G \nabla^2 v \dots \dots \dots (14)$$

Now, differentiating Equations (13) and (14) with respect to x and y, respectively, and adding

$$\rho \left(\frac{\partial^2}{\partial t^2} \left(\frac{\partial u}{\partial x} + \frac{\partial v}{\partial y} \right) \right) = (\lambda + G) \left(\frac{\partial^2 \bar{\epsilon}}{\partial x^2} + \frac{\partial^2 \bar{\epsilon}}{\partial y^2} \right) + G \nabla^2 \left(\frac{\partial u}{\partial x} + \frac{\partial v}{\partial y} \right)$$

or

$$\rho \frac{\partial^2 \bar{\epsilon}}{\partial t^2} = (\lambda + 2G) \nabla^2 \bar{\epsilon} \dots \dots \dots (15)$$

Therefore,

$$\frac{\partial^2 \bar{\epsilon}}{\partial t^2} = \frac{(\lambda + 2G)}{\rho} \nabla^2 \bar{\epsilon} = V_p^2 \cdot \nabla^2 \bar{\epsilon}$$

where

$$V_p = \sqrt{(\lambda + 2G)/\rho}$$

This is the wave equation and shows that the dilatation, $\bar{\epsilon}$ (volumetric strain) is propagated through the medium with velocity, $\sqrt{(\lambda + 2G)/\rho}$, which is referred to as compression wave or P-wave.

On the other hand, differentiating both sides of Equation (13) with respect to y, and of Equation (14) with respect to x,

$$\rho \frac{\partial^2}{\partial t^2} \left(\frac{\partial u}{\partial y} \right) = (\lambda + G) \frac{\partial \bar{\epsilon}}{\partial x \partial y} + G \nabla^2 \left(\frac{\partial u}{\partial y} \right) \dots \dots \dots (16)$$

and

$$\rho \frac{\partial^2}{\partial t^2} \left(\frac{\partial v}{\partial x} \right) = (\lambda + G) \frac{\partial \bar{\epsilon}}{\partial x \partial y} + G \nabla^2 \left(\frac{\partial v}{\partial x} \right) \dots \dots \dots (17)$$

Subtracting Equation (16) from Equation (17) yields,

$$\rho \frac{\partial^2}{\partial t^2} \left(\frac{\partial u}{\partial y} - \frac{\partial v}{\partial x} \right) = G \nabla^2 \left(\frac{\partial u}{\partial y} - \frac{\partial v}{\partial x} \right)$$

Since

$$2\bar{\omega} = \frac{\partial v}{\partial x} - \frac{\partial u}{\partial y} ,$$

therefore,

$$\rho \frac{\partial^2 \bar{\omega}}{\partial t^2} = G \nabla^2 \bar{\omega} \dots \dots \dots (18)$$

or

$$\frac{\partial^2 \bar{\omega}}{\partial t^2} = \frac{G}{\rho} \nabla^2 \bar{\omega} = v_s^2 \nabla^2 \bar{\omega} \dots \dots \dots (19)$$

where

$$v_s = \sqrt{G/\rho}$$

Equation (19) represents the equation for distortional waves and the velocity of propagation is V_s . This is also referred to as the shear wave or S-Wave.

We now consider Rayleigh wave. Let us consider a plane wave through an elastic medium with a plane boundary, and let u and v represent the displacements in the x and y directions, respectively. Therefore,

$$u = \frac{\partial \phi}{\partial x} + \frac{\partial \psi}{\partial y} \dots\dots\dots (20)$$

$$v = \frac{\partial \phi}{\partial y} - \frac{\partial \psi}{\partial x} \dots\dots\dots (21)$$

where ϕ and ψ are two potential functions.

The dilation $\bar{\epsilon}$ can be defined as

$$\bar{\epsilon} = \epsilon_x + \epsilon_y = \frac{\partial u}{\partial x} + \frac{\partial v}{\partial y}$$

or

$$\bar{\epsilon} = \frac{\partial^2 \phi}{\partial x^2} + \frac{\partial^2 \phi}{\partial y^2} = \nabla^2 \phi \dots\dots\dots (22)$$

Similarly, the rotation in the x - y plane can be given by

$$2\bar{\omega} = \frac{\partial u}{\partial y} - \frac{\partial v}{\partial x} = \frac{\partial^2 \psi}{\partial x^2} + \frac{\partial^2 \psi}{\partial y^2} = \nabla^2 \psi \dots\dots\dots (23)$$

Substituting Equations (20) and (22) into Equation (13) yields,

$$\rho \frac{\partial}{\partial x} \left(\frac{\partial^2 \phi}{\partial t^2} \right) + \rho \frac{\partial}{\partial y} \left(\frac{\partial^2 \psi}{\partial t^2} \right) = (\lambda + 2G) \frac{\partial}{\partial x} (\nabla^2 \phi) + G \frac{\partial}{\partial y} (\nabla^2 \psi) \dots\dots\dots (24)$$

Similarly, substituting Equations (21) and (22) into Equation (14) yields,

$$\rho \frac{\partial}{\partial y} \left(\frac{\partial^2 \phi}{\partial t^2} \right) - \rho \frac{\partial}{\partial x} \left(\frac{\partial^2 \psi}{\partial t^2} \right) = (\lambda + 2G) \frac{\partial}{\partial y} (\nabla^2 \phi) - G \frac{\partial}{\partial x} (\nabla^2 \psi) \dots\dots\dots (25)$$

Equations (24) and (25) will be satisfied if :

$$(1) \quad \frac{\partial^2 \phi}{\partial t^2} = \left(\frac{\lambda + 2G}{\rho} \right) \nabla^2 \phi = V_p^2 \cdot \nabla^2 \cdot \phi$$

$$(2) \quad \frac{\partial^2 \psi}{\partial t^2} = \frac{G}{\rho} \cdot \nabla^2 \psi = V_s^2 \cdot \nabla^2 \cdot \psi$$

If we assume

$$\phi = F(y) e^{i(\omega t - fx)} \dots\dots\dots (26)$$

and $\psi = G(y) e^{i(\omega t - fx)} \dots\dots\dots (27)$

where $F(y)$ and $G(y)$ are functions of depths,

$$f = 2 \cdot \pi / \text{wavelength, and}$$

$$i = \sqrt{-1} .$$

Solving Equations (26) and (27) yields,

$$\phi = A \cdot e^{-qy} \cdot e^{i(\omega t - fx)} \dots\dots\dots (28)$$

$$\psi = B \cdot e^{-sy} \cdot e^{i(\omega t - fx)} \dots\dots\dots (29)$$

where

A and B are constants,

$$q = \sqrt{(f^2 - \omega^2 / V_p^2)} \dots\dots\dots (30)$$

$$s = \sqrt{(f^2 - \omega^2 / V_s^2)} \dots\dots\dots (31)$$

Considering boundary conditions of $\sigma_y = 0$ and $\tau_{xy} = 0$ at surface, and combining Equations (20), (21), (28) and (29) yields,

$$16 \left(1 - \frac{\omega^2 \psi}{V_p^2 f^2} \right) \left(1 - \frac{\omega^2}{V_s^2 f^2} \right) = \left(2 - \left(\frac{\lambda + 2G}{G} \right) \frac{\omega^2}{V_p^2 f^2} \right)^2 \left(2 - \frac{\omega^2}{V_s^2 f^2} \right)^2 \dots\dots\dots (32)$$

since $f = \frac{2\pi}{\text{wavelength}}$ or $\text{wavelength} = \frac{2\pi}{f}$, the

wavelength can be defined as,

$$\text{Wavelength} = \frac{\text{velocity of wave } V_r}{(\omega/2\pi)} = \frac{V_r}{(\omega/2\pi)}$$

where V_r is the Rayleigh wave velocity.

Now, let us express V_r in terms of V_s and V_p .

Since $\frac{2\pi}{f} = \frac{2\pi V_r}{\omega}$ or $f = \frac{\omega}{V_r}$

therefore,

$$\frac{\omega^2}{V_p^2 f^2} = \frac{\omega^2}{V_p^2 (\omega^2/V_r^2)} = \frac{V_r^2}{V_p^2} = \alpha^2 V^2 \dots\dots\dots (33)$$

Similarly,

$$\frac{\omega^2}{V_s^2 f^2} = \frac{\omega^2}{V_s^2 (\omega^2/V_r^2)} = \frac{V_r^2}{V_s^2} = V^2 \dots\dots\dots (34)$$

where

$$\alpha^2 = \frac{V_s^2}{V_p^2}$$

However, $V_p^2 = (1/\rho) (\lambda + 2G)$ and $V_s^2 = G/\rho$, therefore,

$$\alpha^2 = \frac{V_s^2}{V_p^2} = \frac{G}{\lambda + 2G} \dots\dots\dots (35)$$

In Hooke's law, poisson's ratio is defined as

$$\nu = \frac{1}{2} \frac{\lambda}{(\lambda + G)} \dots\dots\dots (36)$$

From Equation (36),

$$\lambda = \frac{2 \cdot \nu \cdot G}{(1 - 2\nu)} \dots\dots\dots (37)$$

Substituting Equation (37) into (35) yields,

$$\alpha^2 = \frac{(1 - 2\nu)}{(2 - 2\nu)}$$

Again, substituting Equations (33), (34), and (35) into (32) yields,

$$V^6 - 8V^4 (16\alpha^2 - 24) V^2 - 16(1 - \alpha^2) = 0 \dots\dots\dots (38)$$

This equation can be used to determine the proper value of V^2 in terms of V_p and V_s at a given value of Poisson's ratio. Table 1 shows some values of $V = V_r/V_s$ at various Poisson's ratio.

For displacement of the Rayleigh waves, combining and solving Equations (20), (21), (28), and (29) yields,

$$u = Af_1 \left(-e^{-qy} + \frac{2qs}{s^2 + f^2} e^{-sy} \right) e^{i(\omega t - fx)} \dots\dots\dots (39)$$

and

$$v = Aq \left(-q/f e^{-qy} + \frac{2qf}{s^2 + f^2} e^{-sy} \right) e^{i(\omega t - fx)} \dots\dots\dots (40)$$

TABLE 1. VARIATION OF THE RATIO OF THE RAYLEIGH TO THE SHEAR WAVE FOR VARIOUS POISSON'S RATIO

ν	$V = V_r/V_s$
0.25	0.910
0.29	0.926
0.33	0.933
0.40	0.943
0.50	0.955

If we define the rate of attenuation of the displacement in x and y directions,

$$X(y) = -e^{-(q/f)(fy)} + \left(\frac{2(q/f)(s/f)}{s^2/f^2 + 1} \right) e^{-(s/f)(fy)} \dots\dots (41)$$

$$Y(y) = -\frac{q}{f} e^{-(q/f)(fy)} + \left(\frac{2(q/f)}{s^2/f^2 + 1} \right) e^{-(s/f)(fy)} \dots\dots (42)$$

For example, if we choose a poisson's ratio, $\nu = 0.25$, then

$$X(y) = - e^{(-0.8475 fy)} + 0.5773 e^{(-0.3933 fy)} \dots\dots (43)$$

$$Y(y) = +0.8475 e^{(-0.8475 fy)} - 1.4679 e^{(-0.3933 fy)} \dots\dots (44)$$

Figure 3 shows a nondimensional plot of the variation of the amplitude of vertical and horizontal components of Raleigh waves with depth for various poisson's ratio.

Based on Equations (43) and (44) and Figure 3, the following observation can be made.

1. The magnitude of X decrease rapidly with increasing value of fy . At $fy = 1.21$, X becomes equal to zero; so, at $y = 2\pi/\text{wavelength}$, thus at $y = 1.21/f = 1.21(\text{wavelength})/2\pi = 0.1926$ (wavelength), the value of X is zero. At greater depth, X becomes finite; however it is of the opposite sign, so the vibration takes place in opposite phase.
2. The magnitude of Y first increases with fy , reaches a maximum value at $y = 0.076$ (wavelength) (i.e, $fy = 0.4775$), and then decreases with depth.

C. EQUATION OF MOTION IN AN ELASTIC MEDIUM WITH GRAVITY FORCE

The next consideration is the gravity force in the analysis. On introducing, g , acceleration of gravity in the y direction, into the

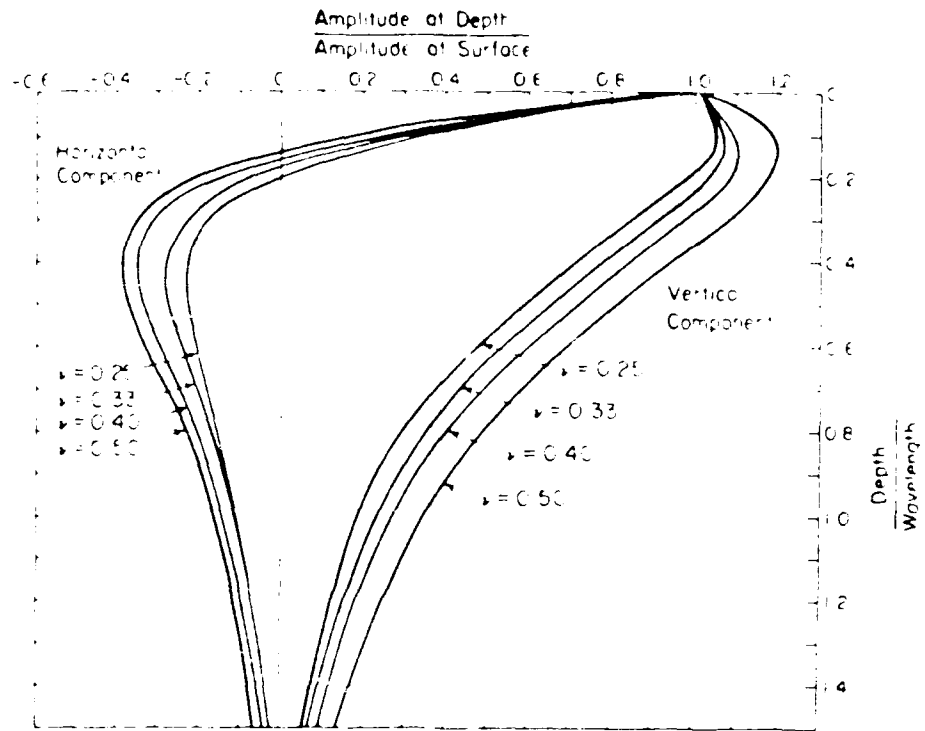


Figure 3. Amplitude Ratio vs. Dimensionless Depth for Rayleigh Wave (Reference 4)

Equations (11) and (12), we obtain

$$\frac{\partial \sigma_x}{\partial x} + \frac{\partial \tau_{xy}}{\partial y} + \rho g \frac{\partial v}{\partial x} = \rho \frac{\partial^2 u}{\partial t^2} \dots\dots\dots (45)$$

$$\frac{\partial \tau_{xy}}{\partial x} + \frac{\partial \sigma_y}{\partial y} + \rho g \frac{\partial v}{\partial y} = \rho \frac{\partial^2 v}{\partial t^2} \dots\dots\dots (46)$$

where u and v are displacement in x and y directions, respectively, and ρ is mass of density. We have assumed the existence of a uniform pressure gradient due to gravity (i.e., the initial hydrostatic pressure distribution). Substituting Hooke's law for an isotropic medium

$$\begin{aligned} \sigma_x &= \lambda \bar{\epsilon} + 2G\epsilon_x \\ \sigma_y &= \lambda \bar{\epsilon} + 2G\epsilon_y \\ \tau_{xy} &= G \cdot \gamma_{xy} \end{aligned}$$

into Equations (45) and (46), we find

$$\rho \frac{\partial^2 u}{\partial t^2} = (\lambda + G) \frac{\partial \bar{\epsilon}}{\partial x} + G \nabla^2 u + \rho g \frac{\partial v}{\partial x} \dots\dots\dots (47)$$

$$\rho \frac{\partial^2 v}{\partial t^2} = (\lambda + G) \frac{\partial \bar{\epsilon}}{\partial y} + G \nabla^2 v + \rho g \frac{\partial v}{\partial y} \dots\dots\dots (48)$$

By differentiating Equations (47) and (48) with respect to x and y ,

respectively, and adding, we obtain

$$\rho \frac{\partial^2}{\partial t^2} \left(\frac{\partial u}{\partial x} + \frac{\partial v}{\partial y} \right) = (\lambda + G) \left(\frac{\partial^2 \bar{\epsilon}}{\partial x^2} + \frac{\partial^2 \bar{\epsilon}}{\partial y^2} \right) + GV^2 \left(\frac{\partial u}{\partial x} + \frac{\partial v}{\partial y} \right) + \rho g \left(\frac{\partial^2 v}{\partial x^2} + \frac{\partial^2 u}{\partial y^2} \right)$$

since

$$\bar{\epsilon} = \left(\frac{\partial v}{\partial x} - \frac{\partial u}{\partial y} \right) \quad \text{and} \quad \bar{\epsilon} = \left(\frac{\partial u}{\partial x} + \frac{\partial v}{\partial y} \right),$$

it follows

$$\rho \frac{\partial^2 \bar{\epsilon}}{\partial t^2} = (\lambda + 2G) \nabla^2 \bar{\epsilon} + \rho g \nabla^2 v \quad \dots \dots \dots (49)$$

On the other hand, by differentiating Equations (47) and (48) with respect to y and x, respectively, and subtracting one from the other we obtain

$$\rho \frac{\partial^2}{\partial t^2} \left(\frac{\partial u}{\partial y} - \frac{\partial v}{\partial x} \right) = (\lambda + G) \left(\frac{\partial \bar{\epsilon}}{\partial x \partial y} - \frac{\partial \bar{\epsilon}}{\partial x \partial y} \right) + GV^2 \left(\frac{\partial u}{\partial y} - \frac{\partial v}{\partial x} \right) + \rho g \frac{\partial}{\partial x} \left(\frac{\partial v}{\partial x} - \frac{\partial v}{\partial y} \right)$$

or

$$\rho \frac{\partial^2 \bar{\omega}}{\partial t^2} = G \nabla^2 \bar{\omega} \quad \dots \dots \dots (50)$$

Equations (49) differs from Equation (15) for a medium without

gravity force. Equation (49) shows the existence of coupling between longitudinal and transversal waves. This coupling is due to the gravity force. The physical meaning of this coupling and the significance of the gravity force in body waves should be investigated. A comprehensive study will be carried out during the subsequent sections.

SECTION III
LABORATORY INVESTIGATION

A. INTRODUCTION

The two-dimensional governing equations of motion in an elastic medium with gravity force in the y direction were given in Equations (45) and (46) They are

$$\frac{\partial \sigma_x}{\partial x} + \frac{\partial \tau_{xy}}{\partial y} + \rho g \frac{\partial v}{\partial x} = \rho \frac{\partial^2 u}{\partial t^2} \dots\dots\dots (51)$$

$$\frac{\partial \tau_{xy}}{\partial x} + \frac{\partial \sigma_y}{\partial y} + \rho g \frac{\partial v}{\partial y} = \rho \frac{\partial^2 v}{\partial t^2} \dots\dots\dots (52)$$

where u and v are displacement in x and y directions, respectively, and ρ is the mass density. By assuming the initial state of stress is hydrostatic and the stress-strain relationship for an isotropic medium obeys the Hooke's law, we obtain

$$\rho \frac{\partial^2 u}{\partial t^2} = (\lambda + G) \frac{\partial \bar{\epsilon}}{\partial x} + G \nabla^2 u + \rho g \frac{\partial v}{\partial x} \dots\dots\dots (53)$$

$$\rho \frac{\partial^2 v}{\partial t^2} = (\lambda + G) \frac{\partial \bar{\epsilon}}{\partial y} + G \nabla^2 v + \rho g \frac{\partial v}{\partial y} \dots\dots\dots (54)$$

Equations (53) and (54) can be simplified by an additional assumption to gain further insight of the roles played by the gravity terms, namely that the material is incompressible. This eliminates the dilatational wave. Hooke's law can then be written for an incompressible material as follows:

$$\sigma_x = -p + 2 \cdot G \cdot \epsilon_x \quad \dots\dots\dots (55)$$

$$\sigma_y = -p + 2 \cdot G \cdot \epsilon_y \quad \dots\dots\dots (56)$$

$$\tau_{xy} = G \cdot \gamma_{xy} \quad \dots\dots\dots (57)$$

where p is the increment of hydrostatic pressure. By substituting, Equations (55), (56) and (57) in Equations (51) and (52) and taking

into account the condition of incompressibility, $\frac{\partial u}{\partial x} + \frac{\partial v}{\partial y} = 0$,

we find

$$\rho \frac{\partial^2 u}{\partial t^2} = G \nabla^2 u - \frac{\partial}{\partial x} (p - \rho g v) \quad \dots\dots\dots (58)$$

$$\rho \frac{\partial^2 v}{\partial t^2} = G \nabla^2 v - \frac{\partial}{\partial y} (p - \rho g v) \quad \dots\dots\dots (59)$$

If one anticipates that the effect of gravity is important, one can derive a dimensionless parameter, which represents the influence of gravity, from Equation (59). This requires

$$G \cdot \nabla^2 \cdot v \sim \rho g \frac{\partial v}{\partial y}$$

$$\text{i.e., } \frac{G \cdot v}{\lambda^2} = \frac{\rho \cdot g \cdot v}{\lambda} \quad \text{or} \quad \frac{\rho \cdot g \cdot \lambda}{G} = 1$$

where λ is the wavelength of the gravity wave. Therefore, the dimensionless gravity parameter $\eta = \rho g \lambda / G$ is the key to the present investigation of gravity effect. After defining a length scale $l = G / \rho g$, the gravity parameter η becomes λ / l . In general, a structure is most vulnerable to the Rayleigh wave when its horizontal length scale is close to half of the wavelength. For instance, $l = 2,570$ feet for a soil with $G = 3,000 \text{ lb/in}^2$ and $\rho g = 168 \text{ lb/ft}^3$. Suppose that the gravity effect is important when $\eta > 0.5$. This corresponds to $\lambda > 1,285$ feet and the horizontal length scale of the structure > 640 feet. That means the structure of that length is vulnerable to the Rayleigh wave enhanced by gravity. This gravity parameter, $\eta = \rho g \lambda / G$, will be varied in the laboratory investigation to see the gravity effects.

Another possible gravity effect may be related to the strength of the initial blast loading. The gravity effect is significant during the initial cratering stage after explosion. The important parameter would be $Q / (G \lambda^3)$, where Q is the impact energy transmitted to the soil.

The two parameters $\rho g \lambda / G$ and $Q / G \lambda^3$, identified above, will be key parameters for our subsequent laboratory investigation.

B. DESCRIPTION OF TESTING FACILITY AND MODEL

The test setup consisted of a drop weight mechanism, a model box, and electronic equipments. A horizontal steel rod that could be adjusted to any desired height was supported by a rigid steel framework. A smooth 1/8-inch diameter steel rod was then fixed vertically to the horizontal rod. The weight was free to slide down the guide when released, and the motion of the falling weight was essentially equivalent to free fall. The weight was cut from an aluminium stock and machined to a close tolerance to allow the guide to pass through it smoothly.

The model box was made of plexiglass, 18 inches in nominal outside diameter and 6 inches high, with the center of the model box positioned directly below the falling weight. The material used in the model tests was commercially available gelatine. The gelatine was first mixed with hot water in a large container, then was carefully poured into the plexiglas model box up to 5 inches high. The model was placed in a cool temperature room for approximately 24 hours. After the mixture was hardened, two pressure transducers were placed on the surface of the medium: one at the center and the other one at a point 6 inches away from the center. The fluid mixture was again poured into the model box to the top of the box, and the model was placed in the cool temperature room for another 24 hours.

The pressure transducers used in the tests were made by the scientists at the General Technology. The transducer was made of

piezoelectric ceramic (see Figure 4). The vertical surface velocity was measured by a magnetic velocity transducer. It consists of a small magnet which moves freely inside a coil. The motion of the magnet will induce a voltage in the coil, similar to an electric generator. The transducer was carefully calibrated against known velocities for quantitative measurements.

Two-channel, type MARK220, special purpose recorder manufactured by the Brush Instruments was used to record the pressure induced in the model by the falling weight. All data before and after impact loading was recorded and printed out on a hard copy. A photograph of the drop weight system, model box filled with the mixture (gelatine), embedded pressure transducers and two-channel recorders is shown in Figure 5.

Seismic methods, including the crosshole, downhole, surface refraction, surface reflection, steady-state Rayleigh-wave method and the spectral-analysis-of-surface-waves(SASW) method, are often used to determine the elastic material properties (i.e., shear modulus, etc.). However, in this experimental study, the shear modulus of the model sample was determined by a different method that was less time consuming and complicated than the seismic methods. Rather, we used a method simple, yet accurate enough to measure the shear modulus of the model. A cube sample with dimensions of 1 inch \times 1 inch \times 1 inch was made of gelatine. The bottom of the sample was fixed, and an incremental shear force was applied on the top surface of the sample by pulling it horizontally through a frictionless pulley. The horizontal small

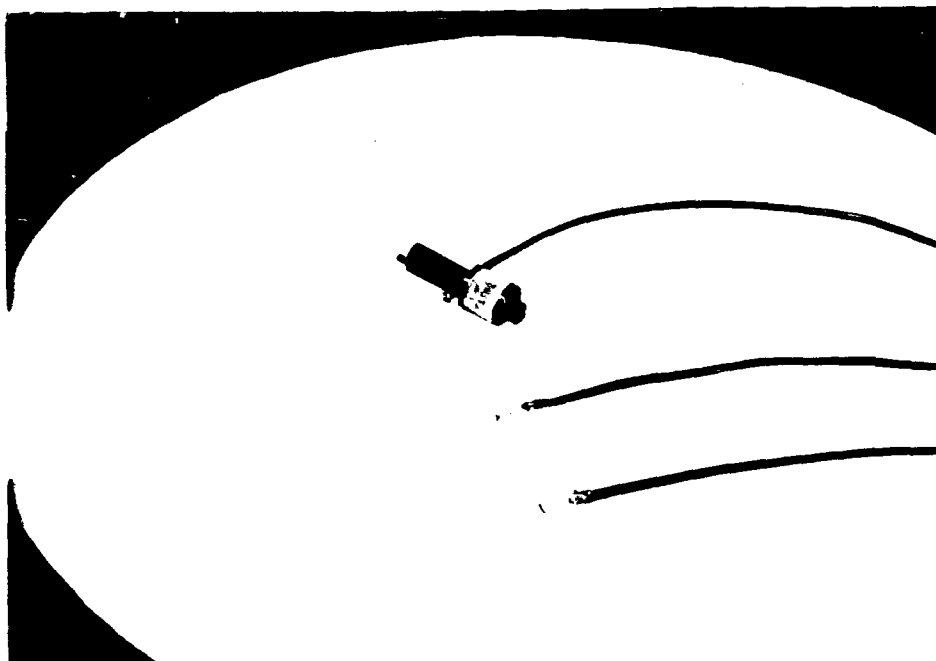


Figure 4. Photograph of Velocity and Pressure Transducers

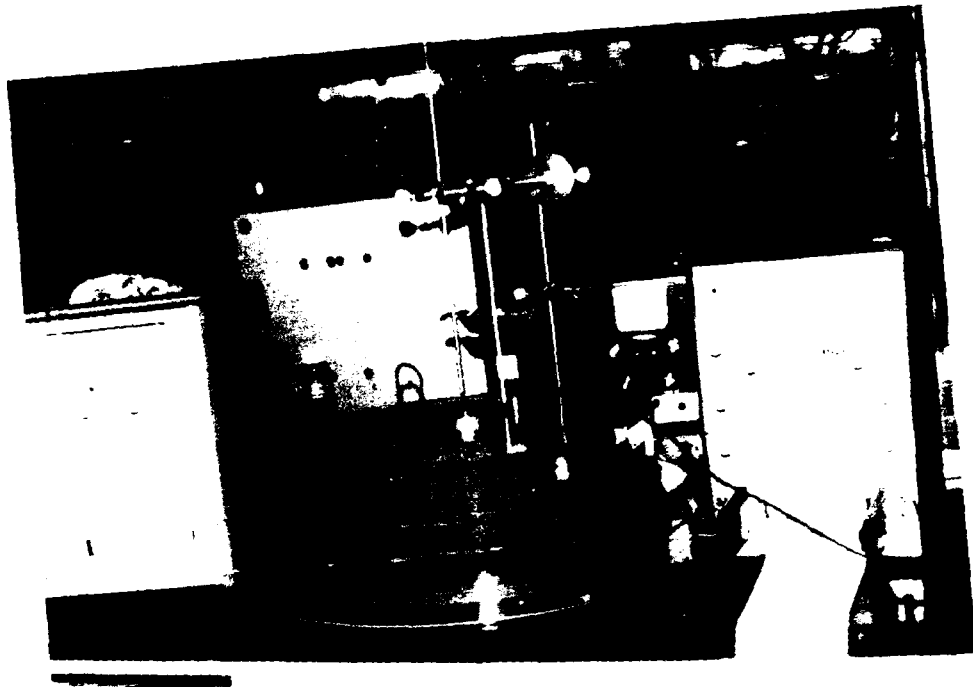


Figure 5. Photograph of a Model, Recorder and Impact Loading System

displacement was measured through a microscope, and corresponding strain was calculated. A photograph of the shear loading apparatus and microscope is shown in Figure 6.

C. LABORATORY PROGRAM

This investigation assumed that the vertical movement of the medium surface due to impact loading of the drop weight would be important. The impact parameter is defined as $Q/(G\lambda^3)$ where $Q = WH$ is the impact energy transmitted to the soil, W is the drop weight, H is the drop height, λ is the wavelength of the Rayleigh wave and G is the shear modulus of the soil. Two different masses (0.2 pound and 0.4 pound) and three different diameters (1 inch., 2 inches., and 3 inches.) of the drop weight (see Figure 7), and six different drop heights (1 inch, 2 inches, 3 inches, 4 inches, 5 inches, and 6 inches.) were chosen as parameters for the experimental model study. Another important parameter to match between the laboratory model and the prototype is the gravity parameter, $\rho g\lambda/G$. This is a measure of the gravity potential energy in relation to the strain energy of the solid medium. To study the significant gravity effects, it is essential that the gravity parameter $\rho g\lambda/G$ be kept at about order one. To achieve this, the shear modulus of the model must be small because of the limited size of the model. As a result, two shear moduli of 0.2 and 1.4 psi were chosen for the laboratory model study. Table 2 shows the parameters considered in the model tests.

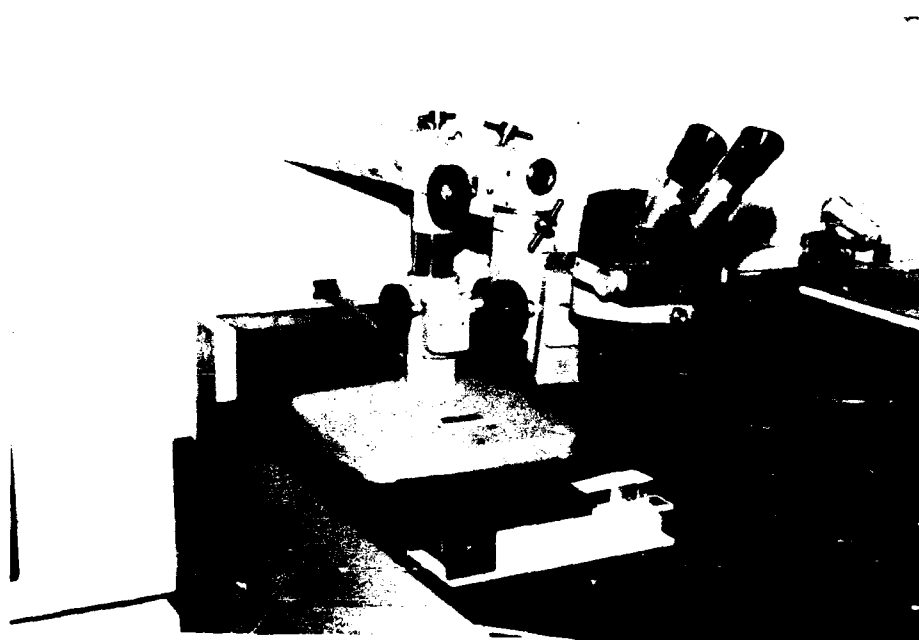


Figure 6. Photograph of Shear Loading Apparatus

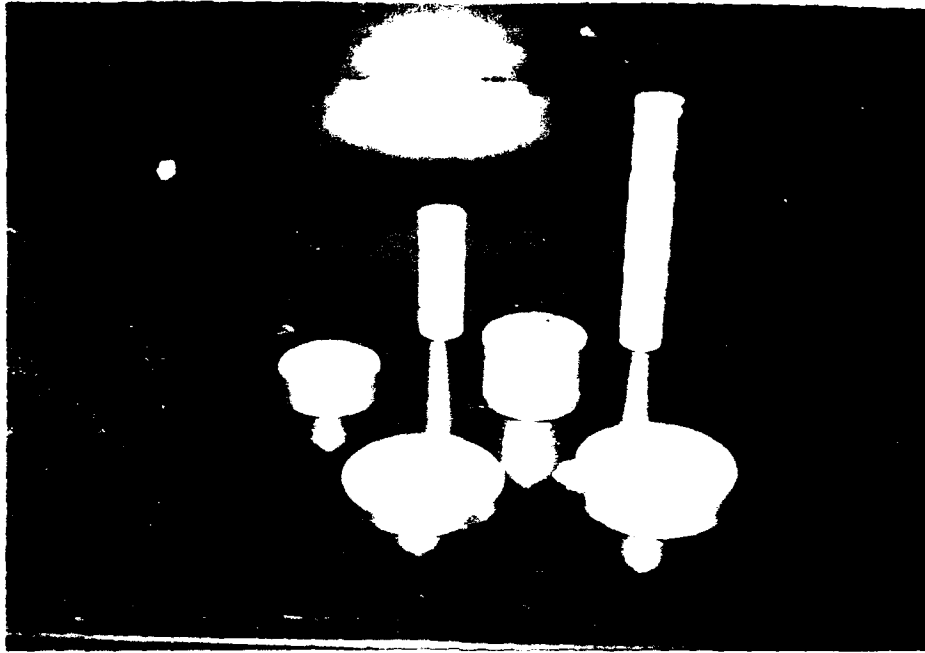


Figure 7. Photograph of Aluminium Drop-Weights

TABLE 2. PARAMETERS CONSIDERED IN THE MODEL TESTS

Parameter	
Shear Modulus of Model	0.2 psi and 1.4 psi
Drop Weight	0.2 lb. and 0.4 lb.
Diameter of Drop Weight	1 in., 2 in., and 3 in.
Drop Height	1 in., 2 in., 3 in., 4 in., 5 in., and 6 in.

SECTION IV
LABORATORY RESULT

A. THE INFLUENCE OF SHEAR MODULUS OF SOLID

Seventy two model tests were performed, and the pressure and velocity responses of the medium under different loading conditions were obtained. Figures 8 and 9 show the typical responses of the pressure and velocity at 1 inch drop height with a 3 inch diameter and 0.4 pound of the drop weight for $G = 0.2$ psi and $G = 1.4$ psi, respectively. Based on the data obtained, frequency, f and period, T , were calculated, and, accordingly, the wave speed, c , and wavelength, λ , were calculated by the following equations :

$$\omega = 2\pi \left(\frac{1}{T}\right)$$

$$c = L/T$$

$$\lambda = c \cdot T$$

where,

ω is the frequency of the harmonic in rad/sec,

T is the period in second,

L is the travel distance in inch,

t is travel time in second,

c is the wave speed in in/sec, and

λ is the wavelength in inch.

The period, T was determined by finding the length at which the waves makes a complete cycle. A few of these cycles make up a group of waves,

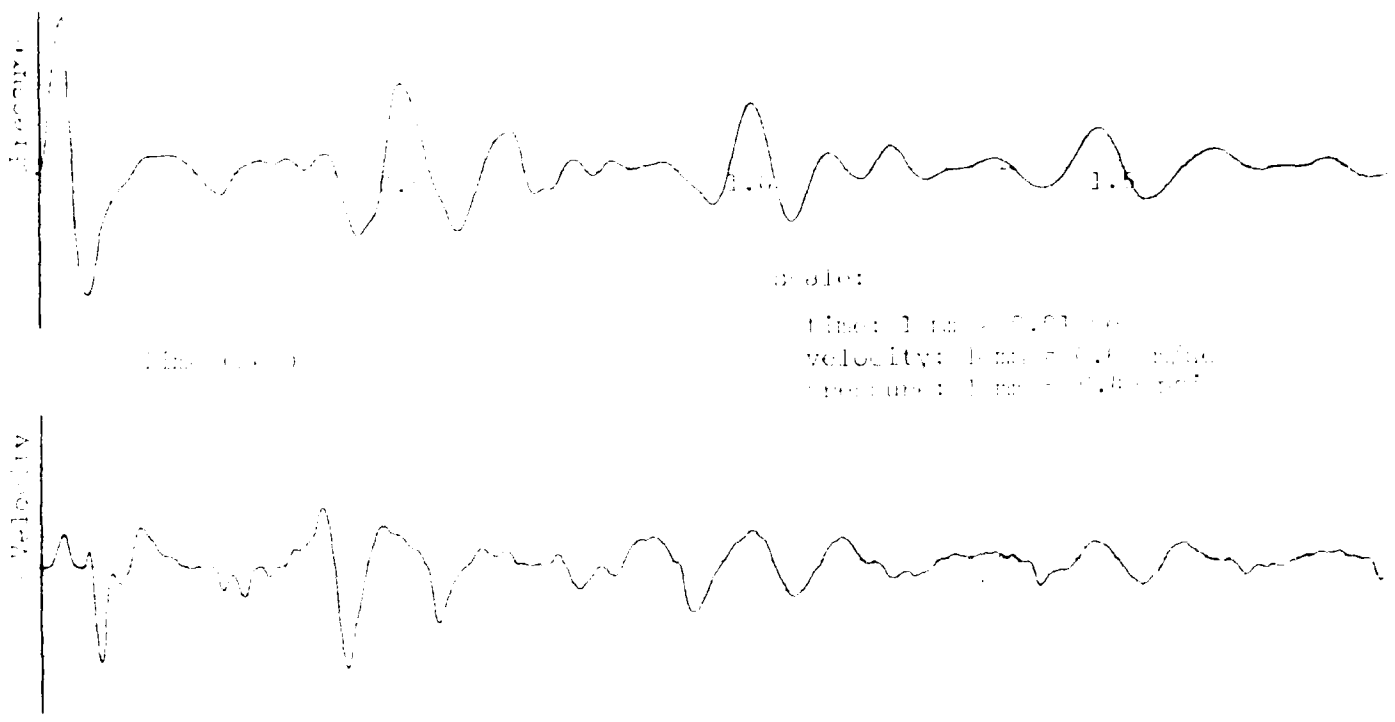


Figure 8. Pressure and Velocity Response for a Model with H=1 in, D=3 in, w=0.1 lb, G=1.4 psi

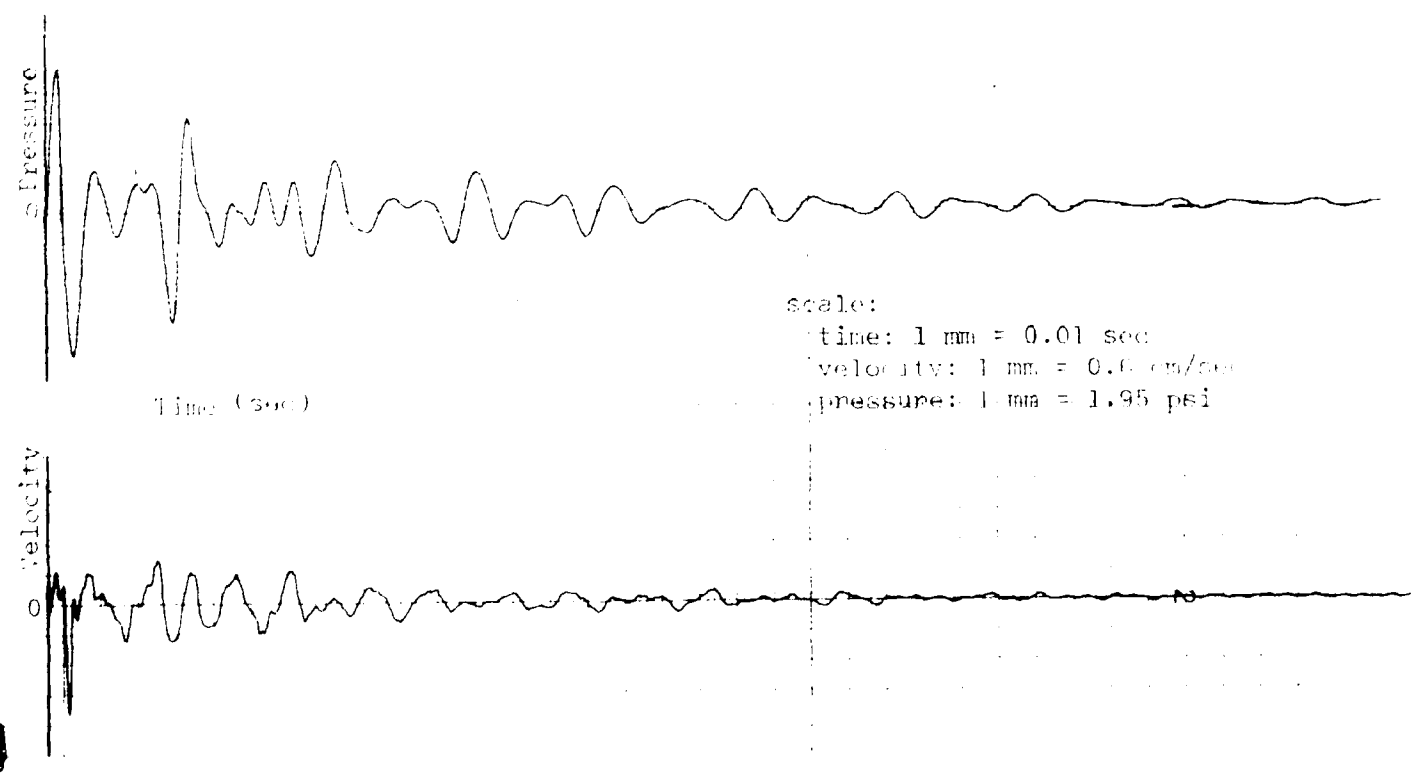


Figure 9. Pressure and Velocity Response for a Model with H=1 in, D=3 in, w=0.4 lb, G=1.4 psi

therefore, the period found was the average of all these values. After the wavelength has been determined, two dimensionless parameters were calculated:

$$\text{gravity parameter} = \rho g \lambda / G$$

$$\text{impact parameter} = W \cdot H / (G \lambda^3)$$

where,

ρ is density of the medium in lb-sec²/in⁴,

g is the acceleration of the gravity, $1 g = 386 \text{ in/sec}^2$,

G is the shear modulus of the medium in psi,

W is the drop weight in pound, and

H is the height of the drop weight in inch.

Tables 3 thru 14 summarize the test results. As shown in Tables 6 and 12, the models failed after 2-inch drop tests. Cracks were developed in the model from high stress concentration caused by heavier weight with small diameter of the drop weight. Also, as shown in Tables 9 and 11, insufficient data were obtained during the model tests due to electrical disconnection in the data acquisition system.

Based on the tables obtained, 10 figures were drawn. Figures 10 and 11 represent a relationship between wave speed and drop height of the weight for models with $G=0.2 \text{ psi}$ and $G=1.4 \text{ psi}$, respectively. It can be observed that wave speed of each model remains almost constant at different drop heights, although with slight variation. Therefore, the wave speed is not a function of the drop height. However, the wave speed is slightly dependent on the diameter of drop weight. The 3-inch

TABLE 3. TEST RESULTS FOR MODEL 1

Shear Modulus, $G = 0.2$ psi
 Drop Weight, $W = 0.2$ lb.
 Diameter of Weight, $D = 1.0$ in.

Drop Height (H)	H = 1 in.	H = 2 in.	H = 3 in.
Density of Model (ρ)	0.906×10^{-4} (lb-sec ² /in ⁴)	0.906×10^{-4} (lb-sec ² /in ⁴)	0.906×10^{-4} (lb-sec ² /in ⁴)
Specific Gravity of Model	0.9694	0.9694	0.9694
Wave Speed (c)	36.3 in/sec	39.0 in/sec	38.0 in/sec
Wavelength (λ)	5.10 in	5.50 in	5.41 in
Gravity Parameter ($\rho g \lambda / G$)	0.893	0.963	0.947
Impact ₃ Parameter ($WH/G\lambda^3$)	0.0075	0.012	0.0190
Maximum Pressure	23.9 psi	40.2 psi	51.1 psi
Maximum Velocity	2.50 in/sec	3.50 in/sec	3.90 in/sec
Drop Height (H)	H = 4 in.	H = 5 in.	H = 6 in.
Density of Model (ρ)	0.906×10^{-4} (lb-sec ² /in ⁴)	0.906×10^{-4} (lb-sec ² /in ⁴)	0.906×10^{-4} (lb-sec ² /in ⁴)
Specific Gravity of Model	0.9694	0.9694	0.9694
Wave Speed (c)	37.3 in/sec	38.5 in/sec	40.6 in/sec
Wavelength (λ)	5.10 in	5.45 in	5.46 in
Gravity Parameter ($\rho g \lambda / G$)	0.893	0.954	0.956
Impact ₃ Parameter ($WH/G\lambda^3$)	0.0301	0.0309	0.0370
Maximum Pressure	54.4 psi	87.0 psi	95.7 psi
Maximum Velocity	3.80 in/sec	4.00 in/sec	4.40 in/sec

TABLE 4. TEST RESULTS FOR MODEL 2

Shear Modulus, $G = 0.2$ psi
 Drop Weight, $W = 0.2$ lb.
 Diameter of Weight, $D = 2.0$ in.

Drop Height (H)	H = 1 in.	H = 2 in.	H = 3 in.
Density of Model (ρ)	0.906×10^{-4} (lb-sec ² /in ⁴)	0.906×10^{-4} (lb-sec ² /in ⁴)	0.906×10^{-4} (lb-sec ² /in ⁴)
Specific Gravity of Model	0.9694	0.9694	0.9694
Wave Speed (c)	40.1 in/sec	43.0 in/sec	40.4 in/sec
Wavelength (λ)	4.20 in	4.25 in	4.49 in
Gravity Parameter ($\rho g \lambda / G$)	0.7350	0.7439	0.7860
Impact Parameter ($WH/G\lambda^3$)	0.0135	0.0261	0.0220
Maximum Pressure	17.4 psi	23.4 psi	30.5 psi
Maximum Velocity	3.00 in/sec	3.90 in/sec	4.40 in/sec
Drop Height (H)	H = 4 in.	H = 5 in.	H = 6 in.
Density of Model (ρ)	0.906×10^{-4} (lb-sec ² /in ⁴)	0.906×10^{-4} (lb-sec ² /in ⁴)	0.906×10^{-4} (lb-sec ² /in ⁴)
Specific Gravity of Model	0.9694	0.9694	0.9694
Wave Speed (c)	40.3 in/sec	42.4 in/sec	43.0 in/sec
Wavelength (λ)	4.48 in	4.70 in	4.60 in
Gravity Parameter ($\rho g \lambda / G$)	0.7840	0.8228	0.805
Impact Parameter ($WH/G\lambda^3$)	0.0445	0.0482	0.0616
Maximum Pressure	39.2 psi	51.1 psi	54.4 psi
Maximum Velocity	4.95 in/sec	5.10 in/sec	5.35 in/sec

TABLE 5. TEST RESULTS FOR MODEL 3

Shear Modulus, $G = 0.2$ psi
 Drop Weight, $W = 0.2$ lb.
 Diameter of Weight, $D = 3.0$ in.

Drop Height (H)	H = 1 in.	H = 2 in.	H = 3 in.
Density of Model (ρ)	0.906×10^{-4} (lb-sec ² /in ⁴)	0.906×10^{-4} (lb-sec ² /in ⁴)	0.906×10^{-4} (lb-sec ² /in ⁴)
Specific Gravity of Model	0.9694	0.9694	0.9694
Wave Speed (c)	45.2 in/sec	45.3 in/sec	45.7 in/sec
Wavelength (λ)	4.38 in	4.39 in	4.37 in
Gravity Parameter ($\rho g \lambda / G$)	0.7670	0.7680	0.7650
Impact ₃ Parameter ($WH/G\lambda^3$)	0.0119	0.0236	0.0359
Maximum Pressure	7.80 psi	9.50 psi	11.9 psi
Maximum Velocity	2.80 in/sec	3.80 in/sec	4.10 in/sec
Drop Height (H)	H = 4 in.	H = 5 in.	H = 6 in.
Density of Model (ρ)	0.906×10^{-4} (lb-sec ² /in ⁴)	0.906×10^{-4} (lb-sec ² /in ⁴)	0.906×10^{-4} (lb-sec ² /in ⁴)
Specific Gravity of Model	0.9694	0.9694	0.9694
Wave Speed (c)	45.6 in/sec	45.3 in/sec	45.6 in/sec
Wavelength (λ)	4.35 in	4.37 in	4.42 in
Gravity Parameter ($\rho g \lambda / G$)	0.761	0.7650	0.774
Impact ₃ Parameter ($WH/G\lambda^3$)	0.0486	0.0599	0.069
Maximum Pressure	14.6 psi	15.2 psi	19.0 psi
Maximum Velocity	4.70 in/sec	4.90 in/sec	5.20 in/sec

TABLE 6. TEST RESULTS FOR MODEL 4

Shear Modulus, $G = 0.2$ psi
 Drop Weight, $W = 0.4$ lb.
 Diameter of Weight, $D = 1.0$ in.

Drop Height (H)	H = 1 in.	H = 2 in.	H = 3 in.
Density of Model (ρ)	0.906×10^{-4} (lb-sec ² /in ⁴)	0.906×10^{-4} (lb-sec ² /in ⁴)	0.906×10^{-4} (lb-sec ² /in ⁴)
Specific Gravity of Model	0.9694	0.9694	0.9694
Wave Speed (c)	42.0 in/sec	48.7 in/sec	*
Wavelength (λ)	6.56 in	7.51 in	*
Gravity Parameter ($\rho g \lambda / G$)	1.185	1.314	*
Impact ₃ Parameter ($WH/G\lambda^3$)	0.0032	0.0047	*
Maximum Pressure	29.4 psi	52.2 psi	*
Maximum Velocity	2.70 in/sec	4.33 in/sec	*

Drop Height (H)	H = 4 in.	H = 5 in.	H = 6 in.
Density of Model (ρ)	0.906×10^{-4} (lb-sec ² /in ⁴)	0.906×10^{-4} (lb-sec ² /in ⁴)	0.906×10^{-4} (lb-sec ² /in ⁴)
Specific Gravity of Model	0.9694	0.9694	0.9694
Wave Speed (c)	*	*	*
Wavelength (λ)	*	*	*
Gravity Parameter ($\rho g \lambda / G$)	*	*	*
Impact ₃ Parameter ($WH/G\lambda^3$)	*	*	*
Maximum Pressure	*	*	*
Maximum Velocity	*	*	*

* : Model Failure

TABLE 7. TEST RESULTS FOR MODEL 5

Shear Modulus, $G = 0.2$ psi
 Drop Weight, $W = 0.4$ lb.
 Diameter of Weight, $D = 2.0$ in.

Drop Height (H)	H = 1 in.	H = 2 in.	H = 3 in.
Density of Model (ρ)	0.906×10^{-4} (lb-sec ² /in ⁴)	0.906×10^{-4} (lb-sec ² /in ⁴)	0.906×10^{-4} (lb-sec ² /in ⁴)
Specific Gravity of Model	0.9694	0.9694	0.9694
Wave Speed (c)	46.2 in/sec	46.1 in/sec	46.9 in/sec
Wavelength (λ)	5.92 in	5.92 in	5.91 in
Gravity Parameter ($\rho g \lambda / G$)	1.036	1.0340	1.034
Impact Parameter ($WH/G\lambda^3$)	0.0096	0.0194	0.0290
Maximum Pressure	25.6 psi	45.7 psi	59.1 psi
Maximum Velocity	3.50in/sec	4.80in/sec	5.40in/sec
Drop Height (H)	H = 4 in.	H = 5 in.	H = 6 in.
Density of Model (ρ)	0.906×10^{-4} (lb-sec ² /in ⁴)	0.906×10^{-4} (lb-sec ² /in ⁴)	0.906×10^{-4} (lb-sec ² /in ⁴)
Specific Gravity of Model	0.9694	0.9694	0.9694
Wave Speed (c)	46.2 in/sec	46.6 in/sec	46.6 in/sec
Wavelength (λ)	5.91 in	5.87 in	5.91 in
Gravity Parameter ($\rho g \lambda / G$)	1.033	1.027	1.034
Impact Parameter ($WH/G\lambda^3$)	0.0390	0.0494	0.0582
Maximum Pressure	80.5 psi	135.9 psi	163.2 psi
Maximum Velocity	5.90in/sec	6.80in/sec	7.70in/sec

TABLE 8. TEST RESULTS FOR MODEL 6

Shear Modulus, $G = 0.2$ psi
 Drop Weight, $W = 0.4$ lb.
 Diameter of Weight, $D = 3.0$ in.

Drop Height (H)	H = 1 in.	H = 2 in.	H = 3 in.
Density of Model (ρ)	0.906×10^{-4} (lb-sec ² /in ⁴)	0.906×10^{-4} (lb-sec ² /in ⁴)	0.906×10^{-4} (lb-sec ² /in ⁴)
Specific Gravity of Model	0.9694	0.9694	0.9694
Wave Speed (c)	48.2 in/sec	48.1 in/sec	48.4 in/sec
Wavelength (λ)	4.44 in	4.44 in	4.43 in
Gravity Parameter ($\rho g \lambda / G$)	0.7772	0.777	0.7754
Impact Parameter ($WH/G\lambda^3$)	0.0456	0.0460	0.1380
Maximum Pressure	14.7 psi	23.0 psi	27.2 psi
Maximum Velocity	3.90 in/sec	5.60 in/sec	5.90 in/sec
Drop Height (H)	H = 4 in.	H = 5 in.	H = 6 in.
Density of Model (ρ)	0.906×10^{-4} (lb-sec ² /in ⁴)	0.906×10^{-4} (lb-sec ² /in ⁴)	0.906×10^{-4} (lb-sec ² /in ⁴)
Specific Gravity of Model	0.9694	0.9694	0.9694
Wave Speed (c)	48.2 in/sec	48.3 in/sec	48.2 in/sec
Wavelength (λ)	4.44 in	4.44 in	4.44 in
Gravity Parameter ($\rho g \lambda / G$)	0.777	0.7772	0.777
Impact Parameter ($WH/G\lambda^3$)	0.0916	0.2284	0.1370
Maximum Pressure	34.8 psi	38.1 psi	48.9 psi
Maximum Velocity	7.10 in/sec	7.70 in/sec	8.20 in/sec

TABLE 9. TEST RESULTS FOR MODEL 7

Shear Modulus, $G = 1.4$ psi
 Drop Weight, $W = 0.2$ lb.
 Diameter of Weight, $D = 1.0$ in.

Drop-Height (H)	H = 1 in.	H = 2 in.	H = 3 in.
Density of Model (ρ)	0.895×10^{-4} (lb-sec ² /in ⁴)	0.895×10^{-4} (lb-sec ² /in ⁴)	0.895×10^{-4} (lb-sec ² /in ⁴)
Specific Gravity of Model	0.9577	0.9577	0.9577
Wave Speed (c)	105.5 in/sec	106.4 in/sec	110.1 in/sec
Wavelength (λ)	5.52 in	5.60 in	5.94 in
Gravity Parameter ($\rho g \lambda / G$)	0.135	0.138	0.147
Impact ₃ Parameter ($WH/G\lambda^3$)	0.0008	0.0016	0.002
Maximum Pressure	60.9 psi	80.1 psi	100.1 psi
Maximum Velocity	1.26 in/sec	1.90 in/sec	3.00 in/sec
Drop Height (H)	H = 4 in.	H = 5 in.	H = 6 in.
Density of Model (ρ)	0.895×10^{-4} (lb-sec ² /in ⁴)	0.895×10^{-4} (lb-sec ² /in ⁴)	0.895×10^{-4} (lb-sec ² /in ⁴)
Specific Gravity of Model	0.9577	0.9577	0.9577
Wave Speed (c)	113.1 in/sec	116.7 in/sec	**
Wavelength (λ)	6.50 in	5.92 in	**
Gravity Parameter ($\rho g \lambda / G$)	0.161	0.146	**
Impact ₃ Parameter ($WH/G\lambda^3$)	0.0021	0.0034	**
Maximum Pressure	135.9 psi	160.1 psi	**
Maximum Velocity	3.60 in/sec	3.80 in/sec	**

** : Insufficient Data

TABLE 10. TEST RESULTS FOR MODEL 8

Shear Modulus, $G = 1.4$ psi
 Drop Weight, $W = 0.2$ lb.
 Diameter of Weight, $D = 2.0$ in.

Drop Height (H)	H = 1 in.	H = 2 in.	H = 3 in.
Density of Model (ρ)	0.895×10^{-4} (lb-sec ² /in ⁴)	0.895×10^{-4} (lb-sec ² /in ⁴)	0.895×10^{-4} (lb-sec ² /in ⁴)
Specific Gravity of Model	0.9577	0.9577	0.9577
Wave Speed (c)	117.9 in/sec	116.8 in/sec	118.9 in/sec
Wavelength (λ)	5.42 in	5.43 in	5.42 in
Gravity Parameter ($\rho g \lambda / G$)	0.1339	0.1342	0.1339
Impact ₃ Parameter ($WH/G\lambda^3$)	0.0010	0.0018	0.0028
Maximum Pressure	55.5 psi	78.9 psi	90.30 psi
Maximum Velocity	2.50 in/sec	3.40 in/sec	3.50 in/sec
Drop Height (H)	H = 4 in.	H = 5 in.	H = 6 in.
Density of Model (ρ)	0.895×10^{-4} (lb-sec ² /in ⁴)	0.895×10^{-4} (lb-sec ² /in ⁴)	0.895×10^{-4} (lb-sec ² /in ⁴)
Specific Gravity of Model	0.9577	0.9577	0.9577
Wave Speed (c)	118.9 in/sec	118.5 in/sec	118.5 in/sec
Wavelength (λ)	5.42 in	5.35 in	5.30 in
Gravity Parameter ($\rho g \lambda / G$)	0.1339	0.1320	0.131
Impact ₃ Parameter ($WH/G\lambda^3$)	0.0036	0.0047	0.0058
Maximum Pressure	104.5 psi	123.1 psi	155.4 psi
Maximum Velocity	3.85 in/sec	4.30 in/sec	4.75 in/sec

TABLE 11. TEST RESULTS FOR MODEL 9

Shear Modulus, $G = 1.4$ psi
 Drop Weight, $W = 0.2$ lb.
 Diameter of Weight, $D = 3.0$ in.

Drop Height (H)	H = 1 in.	H = 2 in.	H = 3 in.
Density of Model (ρ)	0.895×10^{-4} (lb-sec ² /in ⁴)	0.895×10^{-4} (lb-sec ² /in ⁴)	0.895×10^{-4} (lb-sec ² /in ⁴)
Specific Gravity of Model	0.9577	0.9577	0.9577
Wave Speed (c)	122.4 in/sec	**	123.3 in/sec
Wavelength (λ)	4.53 in	**	5.90 in
Gravity Parameter ($\rho g \lambda / G$)	0.1006	**	0.1313
Impact Parameter ($WH/G\lambda^3$)	0.0016	**	0.0020
Maximum Pressure	25.0 psi	**	73.9 psi
Maximum Velocity	2.80 in/sec	**	5.17 in/sec
Drop Height (H)	H = 4 in.	H = 5 in.	H = 6 in.
Density of Model (ρ)	0.895×10^{-4} (lb-sec ² /in ⁴)	0.895×10^{-4} (lb-sec ² /in ⁴)	0.895×10^{-4} (lb-sec ² /in ⁴)
Specific Gravity of Model	0.9577	0.9577	0.9577
Wave Speed (c)	**	123.3 in/sec	**
Wavelength (λ)	**	5.90 in	**
Gravity Parameter ($\rho g \lambda / G$)	**	0.1095	**
Impact Parameter ($WH/G\lambda^3$)	**	0.0060	**
Maximum Pressure	**	78.3 psi	**
Maximum Velocity	**	6.61 in/sec	**

** : Insufficient Data

TABLE 12. TEST RESULTS FOR MODEL 10

Shear Modulus, $G = 1.4$ psi
 Drop Weight, $W = 0.4$ lb.
 Diameter of Weight, $D = 1.0$ in.

Drop Height (H)	H = 1 in.	H = 2 in.	H = 3 in.
Density of Model (ρ)	0.895×10^{-4} (lb-sec ² /in ⁴)	0.895×10^{-4} (lb-sec ² /in ⁴)	0.895×10^{-4} (lb-sec ² /in ⁴)
Specific Gravity of Model	0.9577	0.9577	0.9577
Wave Speed (c)	192.5 in/sec	181.7 in/sec	*
Wavelength (λ)	7.89 in	6.80 in	*
Gravity Parameter ($\rho g \lambda / G$)	0.195	0.168	*
Impact Parameter ($WH/G\lambda^3$)	0.0003	0.0009	*
Maximum Pressure	71.8 psi	122.3 psi	*
Maximum Velocity	2.16 in/sec	3.25 in/sec	*
Drop Height (H)	H = 4 in.	H = 5 in.	H = 6 in.
Density of Model (ρ)	0.895×10^{-4} (lb-sec ² /in ⁴)	0.895×10^{-4} (lb-sec ² /in ⁴)	0.895×10^{-4} (lb-sec ² /in ⁴)
Specific Gravity of Model	0.9577	0.9577	0.9577
Wave Speed (c)	*	*	*
Wavelength (λ)	*	*	*
Gravity Parameter ($\rho g \lambda / G$)	*	*	*
Impact Parameter ($WH/G\lambda^3$)	*	*	*
Maximum Pressure	*	*	*
Maximum Velocity	*	*	*

* - Model Failure

TABLE 13. TEST RESULTS FOR MODEL 11

Shear Modulus, $G = 1.4$ psi
 Drop Weight, $W = 0.4$ lb.
 Diameter of Weight, $D = 2.0$ in.

Drop Height (H)	H = 1 in.	H = 2 in.	H = 3 in.
Density of Model (ρ)	0.895×10^{-4} (lb-sec ² /in ⁴)	0.895×10^{-4} (lb-sec ² /in ⁴)	0.895×10^{-4} (lb-sec ² /in ⁴)
Specific Gravity of Model	0.9577	0.9577	0.9577
Wave Speed (c)	114.8 in/sec	114.8 in/sec	114.8 in/sec
Wave length (λ)	4.44 in	4.85 in	4.80 in
Gravity Parameter ($\rho g \lambda / G$)	0.109	0.1198	0.1186
Impact Parameter ($WH/G\lambda^3$)	0.0032	0.0050	0.0078
Maximum Pressure	67.5 psi	95.7 psi	110.3 psi
Maximum Velocity	4.1 in/sec	4.90 in/sec	5.30 in/sec
Drop Height (H)	H = 4 in.	H = 5 in.	H = 6 in.
Density of Model (ρ)	0.895×10^{-4} (lb-sec ² /in ⁴)	0.895×10^{-4} (lb-sec ² /in ⁴)	0.895×10^{-4} (lb-sec ² /in ⁴)
Specific Gravity of Model	0.9577	0.9577	0.9577
Wave Speed (c)	116.8 in/sec	116.9 in/sec	117.0 in/sec
Wavelength (λ)	4.46 in	4.54 in	5.00 in
Gravity Parameter ($\rho g \lambda / G$)	0.110	0.112	0.124
Impact Parameter ($WH/G\lambda^3$)	0.0129	0.0150	0.0137
Maximum Pressure	150.5 psi	184.9 psi	230.0 psi
Maximum Velocity	5.9 in/sec	6.6 in/sec	7.2 in/sec

TABLE 14. TEST RESULTS FOR MODEL 12

Shear Modulus, $G = 1.4$ psi
 Drop Weight, $W = 0.4$ lb.
 Diameter of Weight, $D = 3.0$ in.

Drop Height (H)	H = 1 in.	H = 2 in.	H = 3 in.
Density of Model (ρ)	0.895×10^{-4} (lb-sec ² /in ⁴)	0.895×10^{-4} (lb-sec ² /in ⁴)	0.895×10^{-4} (lb-sec ² /in ⁴)
Specific Gravity of Model	0.9577	0.9577	0.9577
Wave Speed (c)	120.1in/sec	120.1in/sec	121.1in/sec
Wavelength (λ)	4.99 in	4.99 in	4.95 in
Gravity Parameter ($\rho g \lambda / G$)	0.1233	0.123	0.1223
Impact Parameter ($WH/G\lambda^3$)	0.0044	0.0046	0.014
Maximum Pressure	46.8 psi	60.2 psi	82.4 psi
Maximum Velocity	4.6in/sec	5.65in/sec	7.2in/sec
Drop Height (H)	H = 4 in.	H = 5 in.	H = 6 in.
Density of Model (ρ)	0.895×10^{-4} (lb-sec ² /in ⁴)	0.895×10^{-4} (lb-sec ² /in ⁴)	0.895×10^{-4} (lb-sec ² /in ⁴)
Specific Gravity of Model	0.9577	0.9577	0.9577
Wave Speed (c)	122.6in/sec	122.6in/sec	122.1in/sec
Wavelength (λ)	4.90 in	4.93 in	4.93 in
Gravity Parameter ($\rho g \lambda / G$)	0.121	0.1218	0.122
Impact Parameter ($WH/G\lambda^3$)	0.0128	0.0240	0.0144
Maximum Pressure	93.5 psi	97.9 psi	122.3 psi
Maximum Velocity	8.1in/sec	8.41in/sec	9.01in/sec

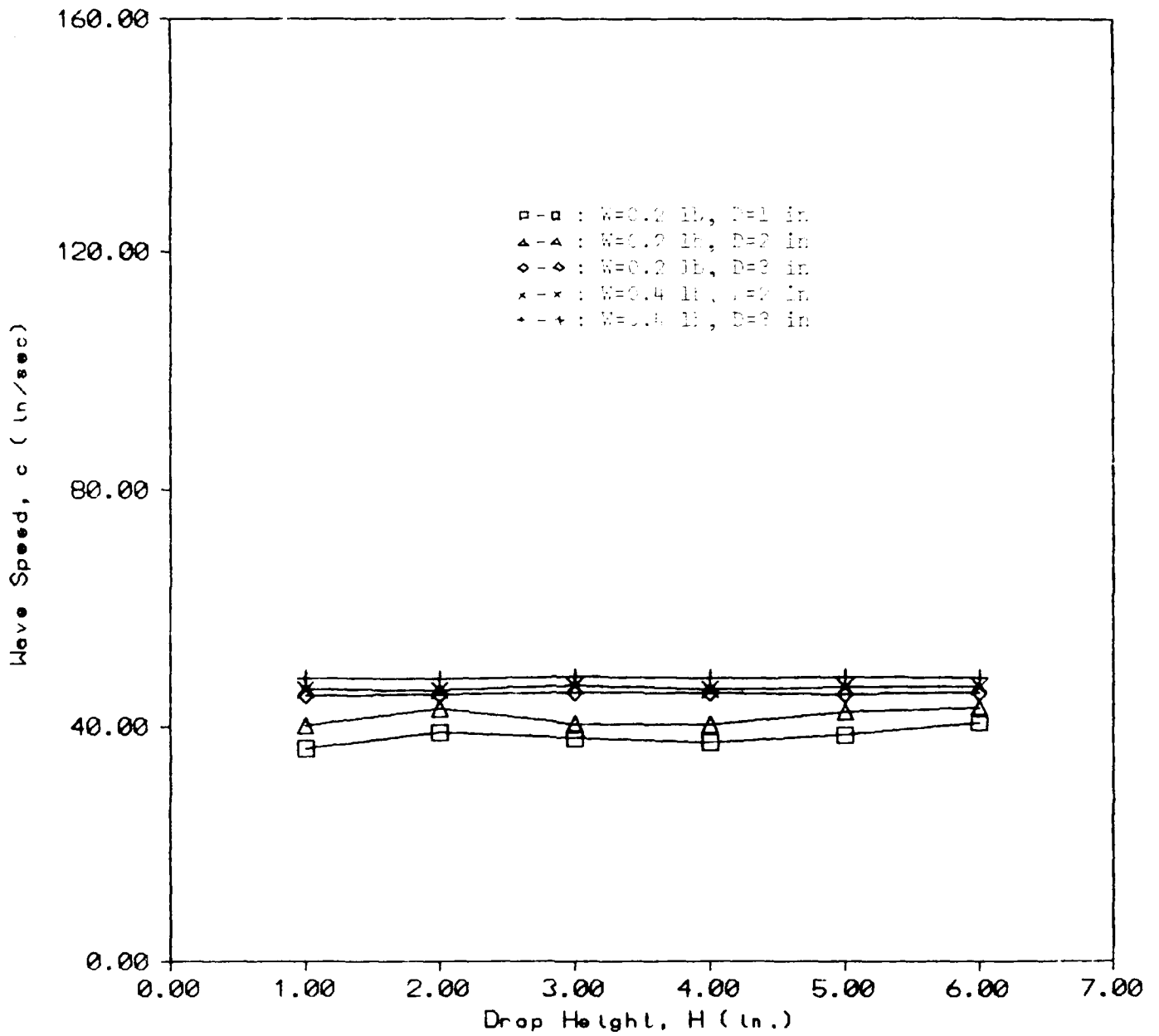


Figure 10. Wavelength vs. Drop Height for Models with G=0.2 psi

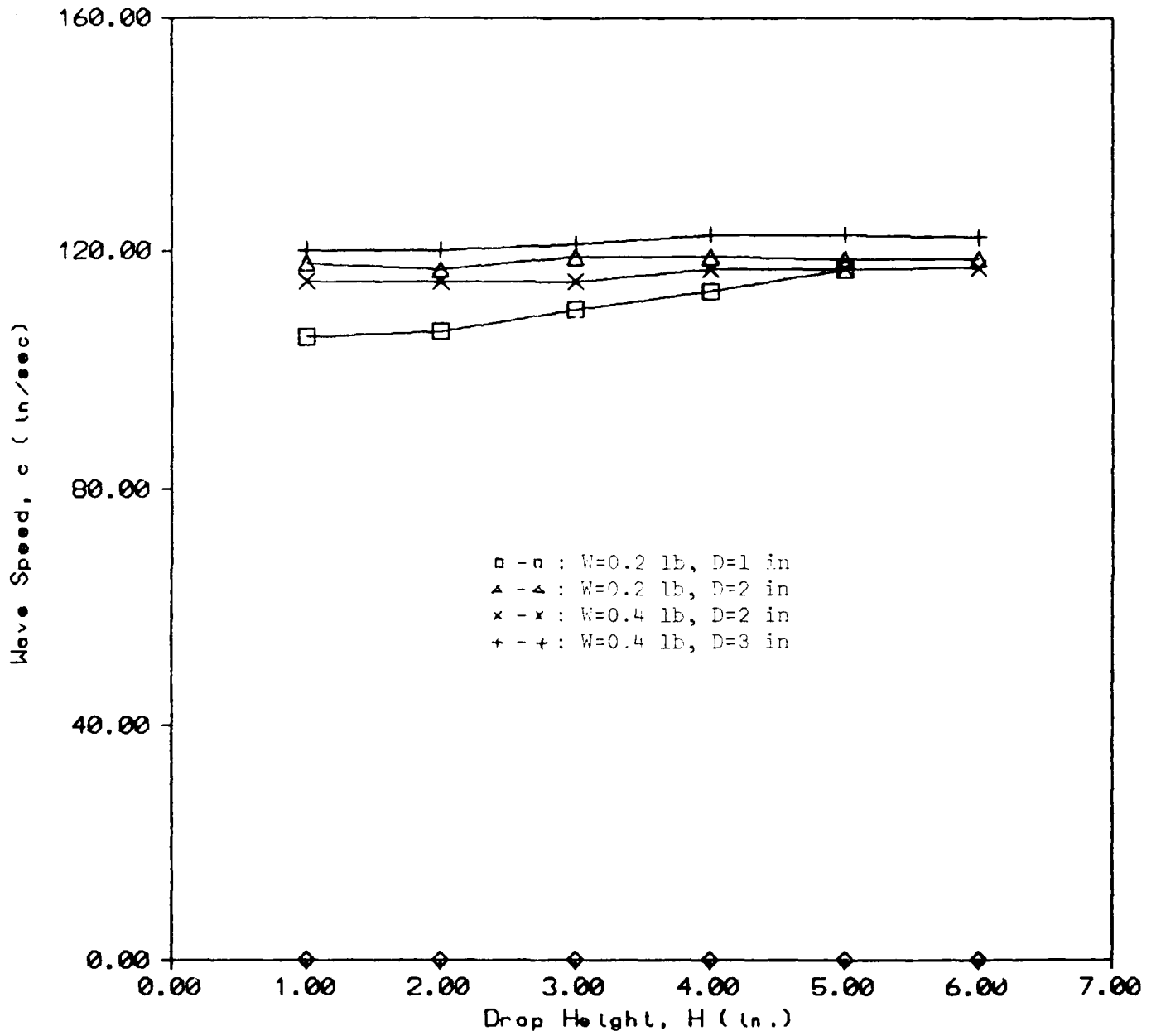


Figure 11. Wavelength vs. Drop Height for Models with G=1.4 psi

diameter drop weight induces the highest wave speed while the 1-inch diameter drop weight induces the lowest wave speed, and may, thus indicate the influence of cratering sizes on Rayleigh's wave speed. However, the size of the cratering is coupled with impact and explosion energy, thereby, impact loadings and explosion energies are important factors in practice. As expressed earlier, a higher wave speed was obtained when a higher shear modulus (1.4 psi) of the medium was used. It confirms the influence of shear modulus on propagating wave speed.

Figures 12 and 13 show a relationship between wavelength and drop height of the drop weight for models with $G = 0.2$ psi and $G = 1.4$ psi, respectively. First observation from the figure again, shows the independency of the wavelength from the drop height. Second observation is that the magnitude of the wavelength are between 4 to 6 inches for all tests. However, it is very difficult to define the parameters that influence the differences in wavelength magnitude. It is certainly due to period, T , and wave speed which is, in turn, related to the diameter of the drop weight.

Figures 14 and 15 represent a relationship between two dimensionless parameters, $\rho g \lambda / G$ and $\rho g D / G$, for models with $G = 0.2$ psi and $G = 1.4$ psi. The wavelength is dependent on the diameter of the drop weight; however, this dependence on the diameter is very slight when $W = 0.2$ pound. It also shows that the dependence on the drop height is insignificant.

The maximum pressure recorded by the pressure transducer at the

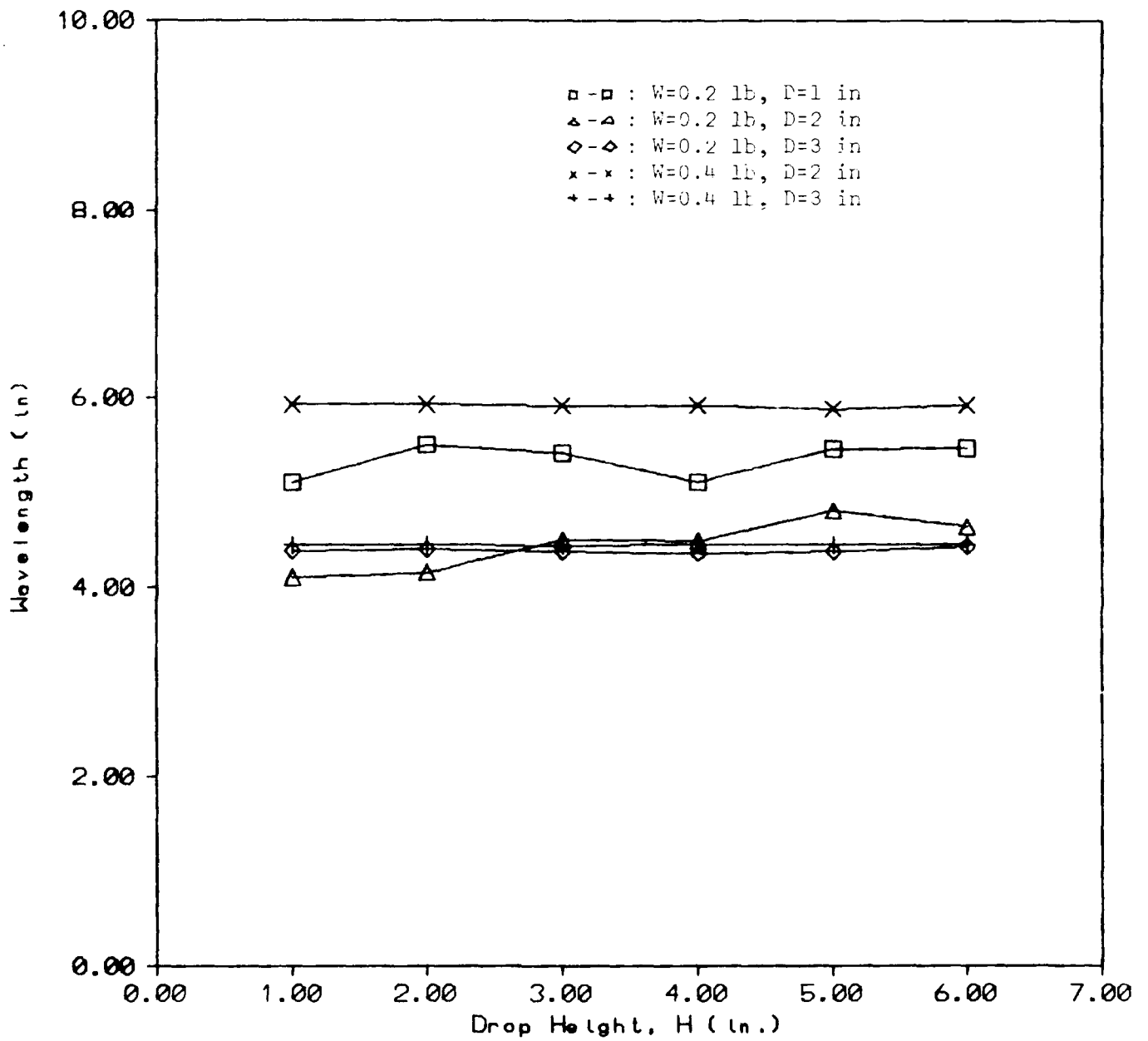


Figure 12. Wave Speed vs. Drop Height for Models with G=0.2 psi

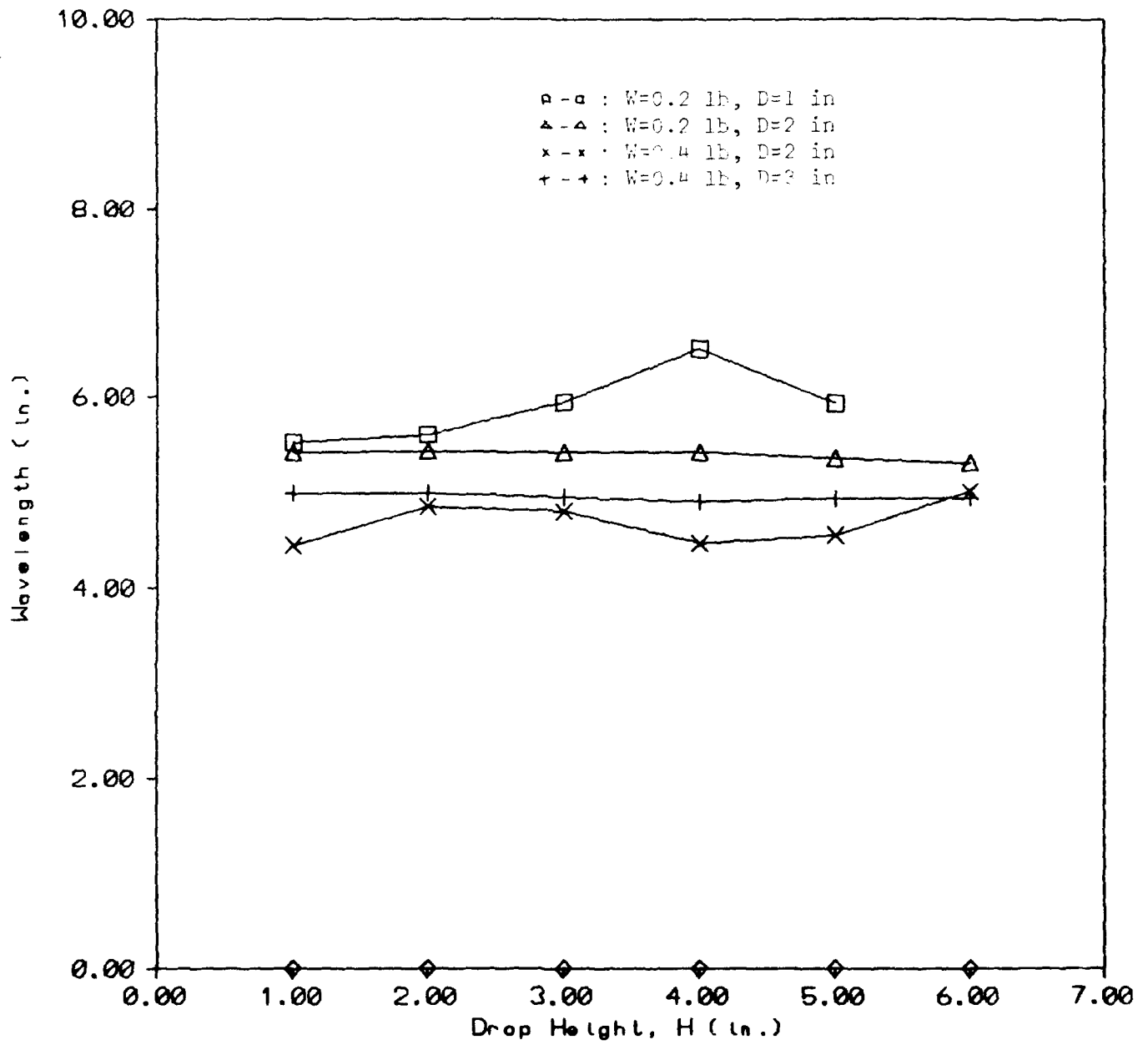


Figure 13. Wave Speed vs. Drop Height for Models with $G=1.4$ psi

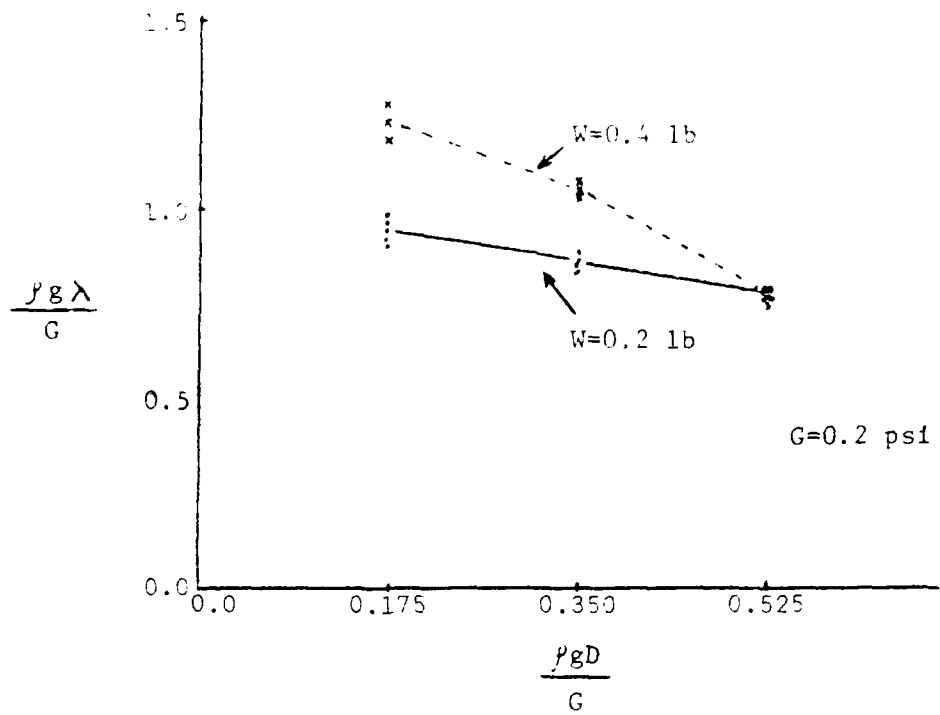


Figure 14. A Relationship of Dimensionless Parameters for Models

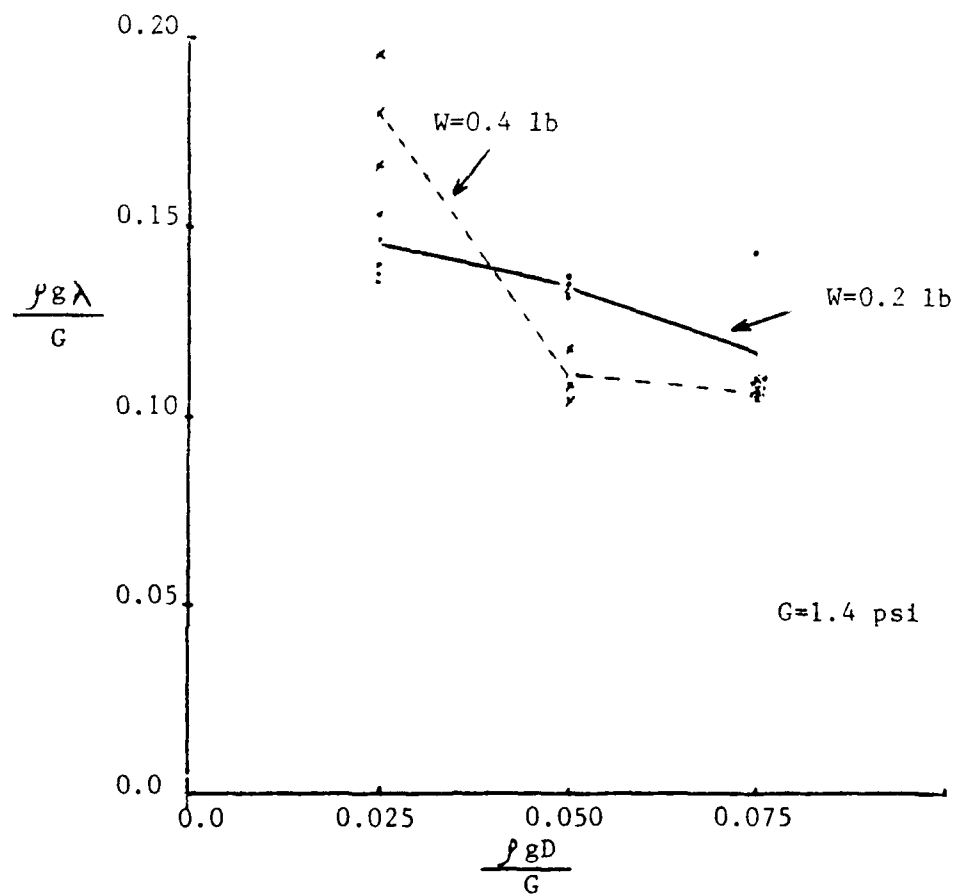


Figure 15. A Relationship of Dimensionless Parameters for Models

center represents the degree of impact as well as the magnitude of deformation at that particular location. Another indication of the magnitude of deformation of the medium caused by impact loading is represented by the maximum vertical velocity recorded by the off-center velocity transducer at the surface.

Figures 16 and 17 show the relationship between the maximum pressure, P and the impact energy, WH . The results show that the maximum pressure has a linear relationship with the impact energy, WH , and, as expected, the smaller diameters induce higher maximum pressures at a given energy due to the smaller contact area.

Figures 18 and 19 show the relationship between the maximum vertical velocity of the medium on the surface and the impact energy, WH , for both cases $G = 0.2$ psi and 1.4 psi. As shown in Figures 10 and 11 for the wavespeed, the vertical velocity is coupled with the diameter of the drop weight. The 3-inch diameter drop weight induces the highest vertical velocity while 1-inch diameter drop weight induces the lowest vertical velocity for all cases. The results also show the linear dependence on WH for most cases. The magnitudes of the velocity vary from 1 to 9 in/s.

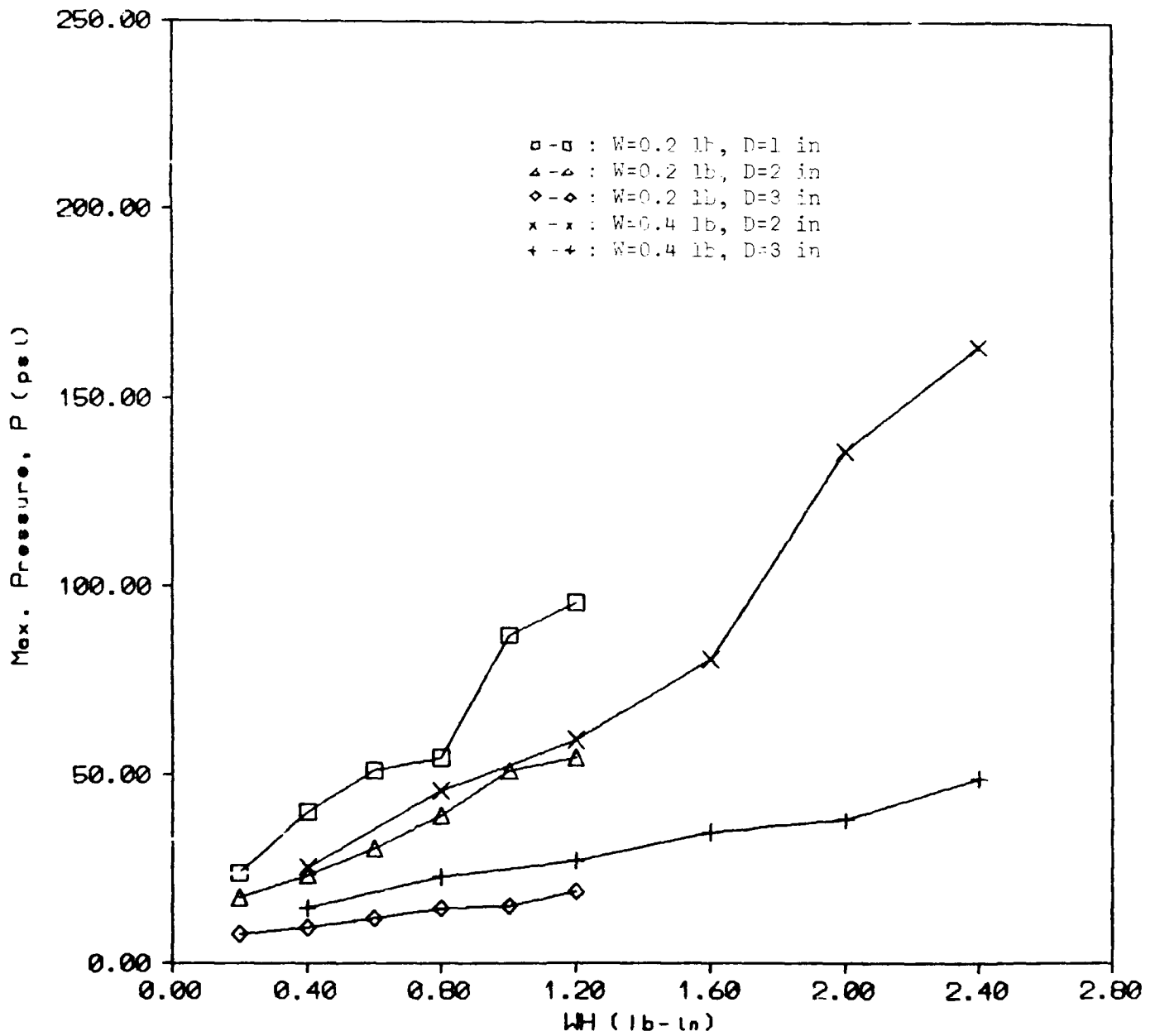


Figure 16. Maximum Pressure vs. Impact Energy for Models with G=0.2 psi

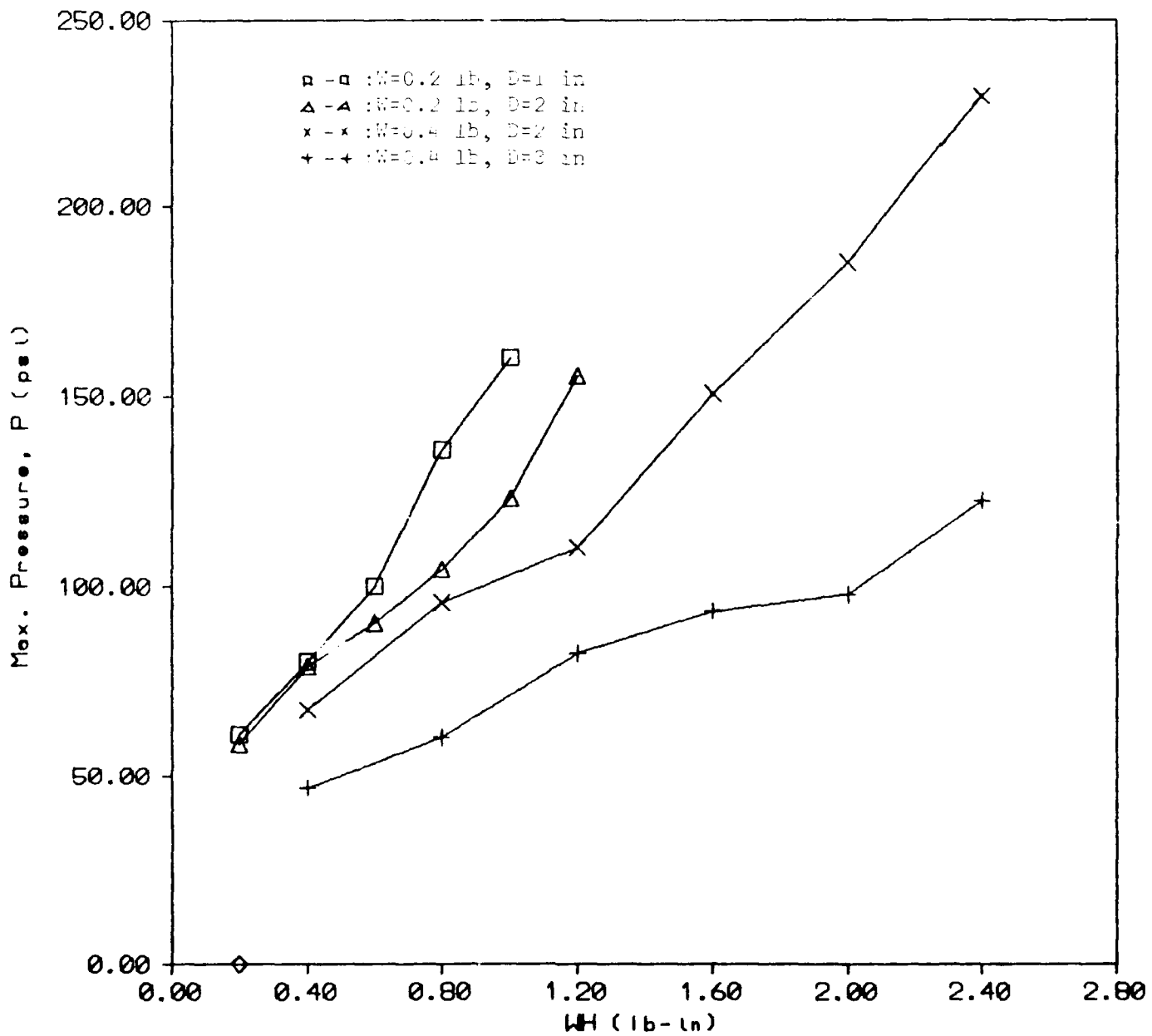


Figure 17. Maximum Pressure vs. Impact Energy for Models with G=1.4 psi

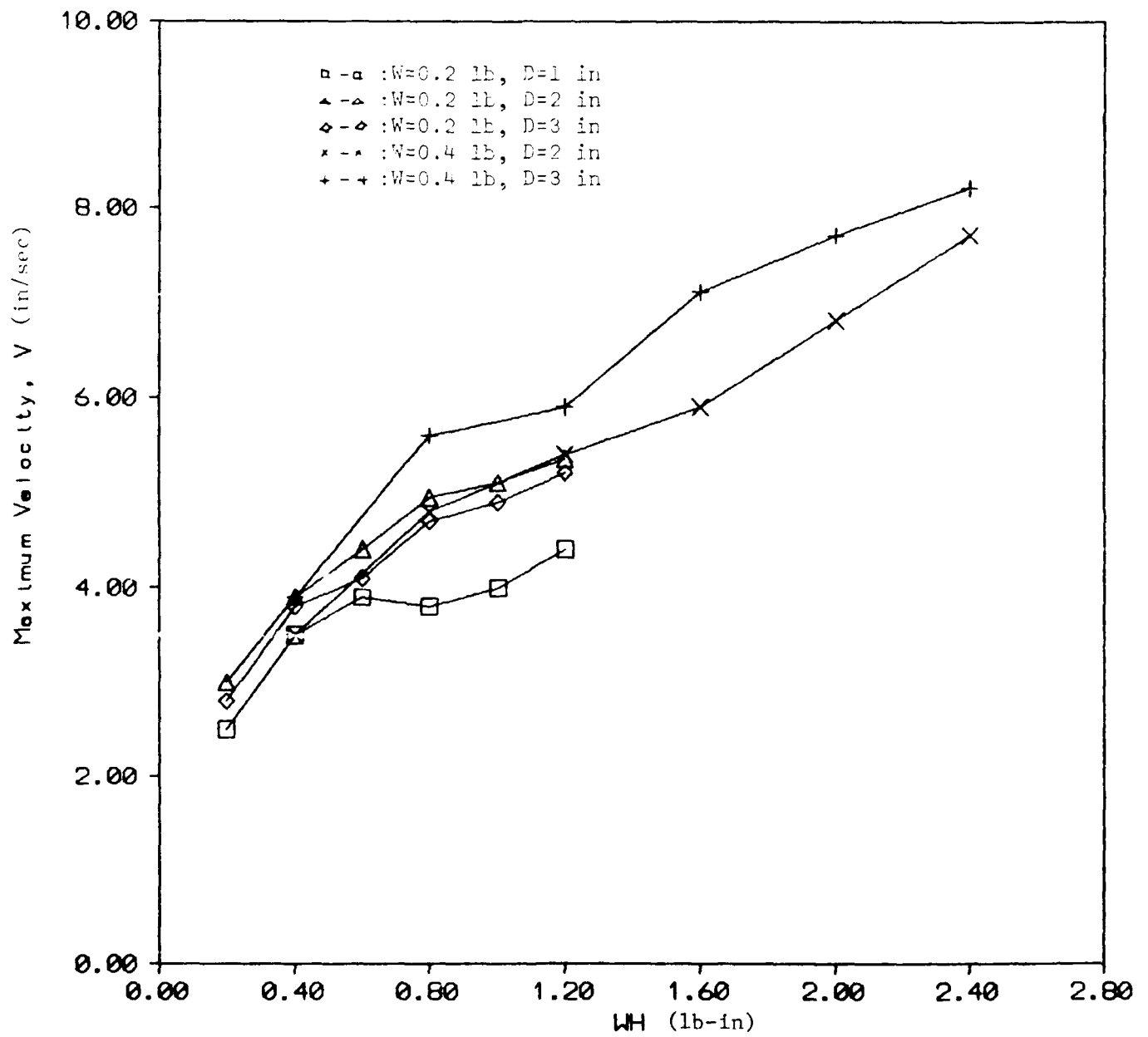


Figure 18. Maximum Velocity vs. Impact Energy for Models with G=0.2 psi

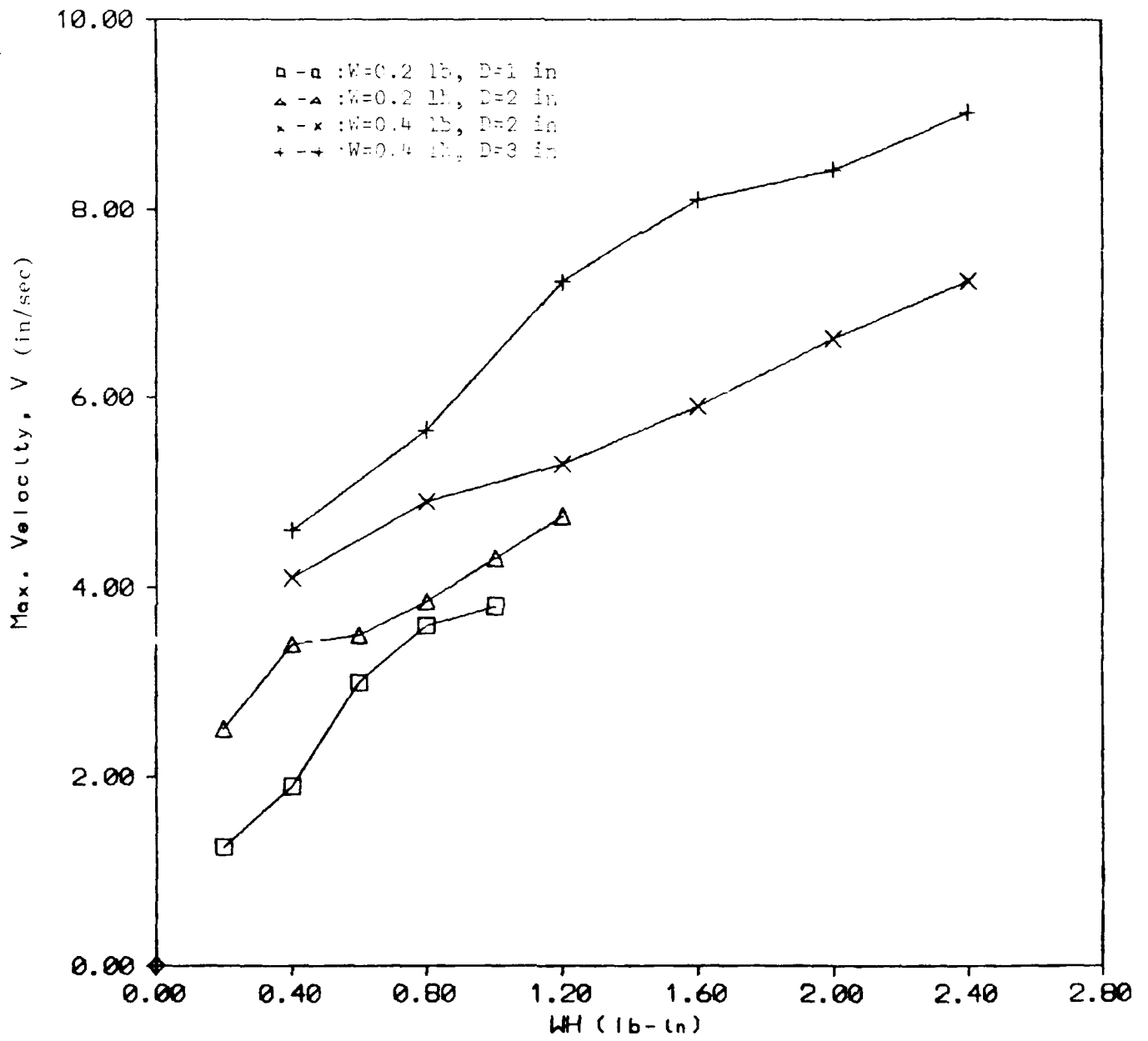


Figure 19. Maximum Velocity vs. Impact Energy for Models with G=1.4 psi

SECTION V

CONCLUSIONS AND RECOMMENDATIONS

A. CONCLUSIONS

The following conclusions were drawn from the analysis of the equation of motion in an elastic medium with gravity force and the laboratory investigation performed.

1. Wave speed, c , is constant and independent of the drop height, H , at a given diameter of the drop weight. However, wave speed increases slightly when the diameter of the drop weight, W , increases.

2. The wavelength is virtually independent of the drop height at a given diameter of the drop weight. The wavelength is decreased while diameter of the weight increases. This is shown contradictory to our intuition that the wavelength would be larger due to larger contact areas. Further investigation is needed for clearer understanding on this phenomenon.

3. The governing parameter in this study is the gravity parameter, $\rho g \lambda / G$. The gravity effect is prominent when the gravity parameter is of order of 1 or larger. It is a function of the intensity of ground movement which is related to the intensity of vertical displacement due to impact loadings. When gravity effect is important, the scaling length for ground movement is $l = G / \rho g$.

4. Gravity parameter, $\rho g \lambda / G$, varies from 0.72 to 1.00 for a model with shear modulus, $G = 0.2$ psi and from 0.12 to 0.14 for a model with $G = 1.4$ psi. It indicates that the use of a model with large shear modulus is not adequate to investigate the gravity effects since the model is too stiff, thereby, small surface movement is induced.

5. The governing parameter $\rho g \lambda / G$ is uniquely related to another parameter $\rho g D / G$ under impact loading. Therefore, there would be a relationship between the wave length, λ and the diameter of the drop weight, D . Further investigation is needed to study these relationships.

6. The important parameters in this study are related to three important controlling parameters : density, gravity and shear modulus. Thus, it may lead us to three options to simulate the gravity effects in small scale modeling : controlling density (ρ), gravity (g) and shear modulus (G).

B. RECOMMENDATIONS

This project raised the possibility of further research topics relating to the gravity effects in small-scale modeling.

1. Since the initial intent of this study was to determine the parameters that govern the gravitational effects, future efforts should consider different magnitude of the each gravity parameter for more comprehensive study.

2. Additional work should be performed to investigate the effects of gravity parameters in a model with a small-scale structure. This will help to determine the feasibility of controlling gravity parameters in small-scale modeling.

3. The gravity-controlled small-scale model study without using the centrifuge techniques should be supplemented by a centrifuge model study for comparison purpose.

4. A field study is necessary to verify the results of the centrifuge model study and gravity-controlled small-scale model study once reasonable information is obtained.

REFERENCES

1. Baker, W. F., Westine, P. S., and Dodge, F. T., Similarity Method in Engineering Dynamics, Hayden Book Company, Inc., Rochelle Park, New Jersey, 1973.
2. Biot, M. A., The Influence of Initial Stress on Elastic Waves, Journal of Applied Science, Vol. 11, No. 8, 1940.
3. Das, B. M., Fundamentals of Soil Dynamics, Elsevier Science Publishing Co., Inc, New York, New York, 1983.
4. Kutter, B. L., O'Leary, L.M. and Thompson, P. Y., "Centrifugal Modelling of the Effect of Blast Loading," Presentation of Second Symposium on the Interaction of Non-Nuclear Munitions with Structures, Panama City Beach, Florida, 1985.
5. Lamb, H., "On the Propagation of Tremors over the Surface of an Elastic Solid," Philosophical Transactions of the Royal Society, London, Ser. A, Vol. 203, 1904.
6. Langhar, H. L. Dimensional Analysis and Theory of Models, Robert E. Krieger Publishing Co., Malabar, Florida, 1983.
7. Murphy, G., Similitude in Engineering, Ronald Press Co., New York, New York, 1950.
8. Nielson, J. P., The Centrifuge Simulation of Blast Parameters, Report No. ESI-TR-83-12, Air Force Engineering and Services Center, Tyndall AFB, 1983.
9. Richart, F.E., H 11, J.R. and Woods, R. D., Vibrations of Soils and Foundations, Prentice-Hall, Inc., Englewood Cliffs, New Jersey, 1970.
10. Schmidt, R. M., and Hopsapple, K. A., Centrifuge Crater Scaling Experiment II, Boeing Aerospace Company, Seattle, Washington, May, 1979.
11. Townsend, F. C., McVay, M. C., and Bradley, D. M., Cunningham, C. H. and Yovaish, D. J., "Numerical and Centrifugal Modelling of Buried Structure Response to Near Blast," Proceedings of Second Symposium on the Interaction of Non-Nuclear Munitions with Structures, Panama City Beach, Florida, 1985.